

Entanglement Polytopes: Multiparticle Entanglement from Single-Particle Information

Michael Walter,¹ Brent Doran,² David Gross,³ and Matthias Christandl¹

¹*Institute for Theoretical Physics, ETH Zurich, Wolfgang–Pauli–Strasse 27, CH-8093 Zurich, Switzerland*

²*Department of Mathematics, ETH Zurich, Rämistrasse 101, CH-8092 Zurich, Switzerland*

³*Institute for Physics, University of Freiburg, Rheinstrasse 10, D-79104 Freiburg, Germany*

Entangled many-body states are an essential resource for quantum computing and interferometry. Determining the type of entanglement present in a system usually requires access to an exponential number of parameters. We show that in the case of pure multi-particle quantum states, features of the global entanglement can already be extracted from local information alone. This is achieved by associating with any given class of entanglement an entanglement polytope—a geometric object which characterizes the single-particle states compatible with that class. Our results, applicable to systems of arbitrary size and statistics, give rise to local witnesses for global pure-state entanglement, and can be generalized to states affected by low levels of noise.

Entanglement is a uniquely quantum mechanical feature. It is responsible for fundamentally new effects—such as quantum non-locality—and constitutes the basic resource for concrete tasks such as quantum computing (1) and interferometry beyond the standard limit (2, 3). Considerable efforts have been directed at obtaining a systematic characterization of multi-particle entanglement; however, our understanding remains limited as the complexity of entanglement scales exponentially with the number of particles (4).

In this work, we show that, for pure quantum states, single-particle information alone can serve as a powerful witness to multi-particle entanglement. In fact, we find that a finite list of linear inequalities characterizes the eigenvalues of the single-particle states in any given class of entanglement. Their violation provides a criterion for witnessing multi-particle entanglement that (i) only requires access to a linear number of degrees of freedom, (ii) applies universally to quantum systems of arbitrary size and statistics, and (iii) distinguishes among many important classes of entanglement, including genuine multi-particle entanglement. Geometrically, these inequalities cut out a hierarchy of polytopes, which captures all information about the global pure-state entanglement deducible from local information alone. Our methods are sufficiently robust to be applicable to situations where the state is affected by low levels of noise.

Formally, a pure state is said to be entangled if it cannot be written as a product $|\psi^{(1)}\rangle \otimes \dots \otimes |\psi^{(N)}\rangle$ (4). Two states can be considered to belong to the same entanglement class if they can be converted into each other with finite probability of success using local operations and classical communication (stochastic LOCC, or SLOCC) (5, 6). For small systems, these entanglement classes are well-understood. In the simplest scenario of three qubits (two-level systems), there exist two classes of genuinely entangled states of very different nature: the first contains the famous Greenberger–Horne–Zeilinger (GHZ) state $\frac{1}{\sqrt{2}}(|\uparrow\uparrow\uparrow\rangle + |\downarrow\downarrow\downarrow\rangle)$, which exhibits a particularly strong form of quantum correlations (7); the second contains the W state $\frac{1}{\sqrt{3}}(|\uparrow\uparrow\downarrow\rangle + |\uparrow\downarrow\uparrow\rangle + |\downarrow\uparrow\uparrow\rangle)$ (6). Whereas states in the W class can be approximated to arbitrary precision by states from the GHZ class, the converse is not true—implying stronger entanglement of the GHZ class (6). Already for four particles there exist infinitely many entanglement classes (8), and the number of parameters required to determine the class

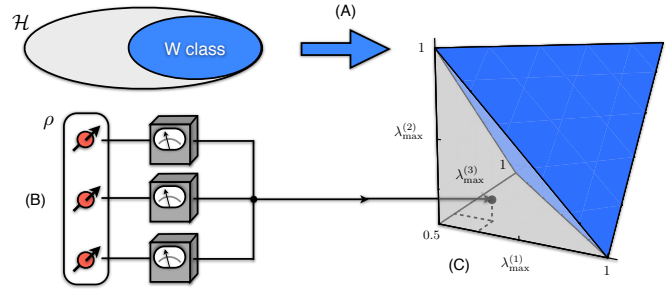


Figure 1. *Entanglement polytopes as witnesses (illustrated for three qubits).* (A) An entanglement polytope contains all possible local eigenvalues of states in the entanglement class (the W class and its polytope are shown in blue). (B) For a sufficiently pure quantum state ρ , local tomography is performed to determine its local eigenvalues. (C) The indicated eigenvalues are not compatible with the W class, hence ρ must have GHZ-type entanglement.

grows exponentially with the particle number. As a result, only sporadic results have been obtained for larger systems, despite the enormous amount of literature dedicated to the problem (4).

Our approach to multi-particle entanglement is based on establishing a connection to the one-body quantum marginal problem, or N -representability problem in quantum chemistry. This fundamental problem about quantum correlations asks which single-particle density matrices $\rho^{(1)}, \dots, \rho^{(N)}$ can appear as the reduced density matrices of a globally pure quantum state. Its solution is easily seen to depend only on the eigenvalues $\vec{\lambda}^{(k)}$ of the densities and allows for an elegant mathematical description: the set of possible vectors $\vec{\lambda} = (\vec{\lambda}^{(1)}, \dots, \vec{\lambda}^{(N)})$ forms a convex polytope (9–11) whose defining inequalities can be computed algorithmically (10, 11). For fermions, the most famous such inequality is the Pauli principle (12, 13).

Here we make the crucial observation that these local eigenvalues alone can already give considerable information about the entanglement of the global state, provided that it is pure. To make this precise, we consider the set of all eigenvalue vectors $\vec{\lambda}$ of the states in the closure of a given entanglement class. Surprisingly, this set also forms a convex polytope (i.e., it is the convex hull of finitely many such vectors), and we call it the entanglement polytope of the class. Entanglement polytopes

immediately lead to a local criterion for witnessing global multi-particle entanglement: If the collection of eigenvalues $\vec{\lambda} = (\vec{\lambda}^{(1)}, \dots, \vec{\lambda}^{(N)})$ of the single-particle reduced density matrices of a pure quantum state $|\psi\rangle$ does not lie in an entanglement polytope $\Delta_{\mathcal{C}}$, then the given state cannot belong to the corresponding entanglement class \mathcal{C} (Fig. 1). Mathematically,

$$\vec{\lambda} = (\vec{\lambda}^{(1)}, \dots, \vec{\lambda}^{(N)}) \notin \Delta_{\mathcal{C}} \implies |\psi\rangle \notin \mathcal{C}. \quad (1)$$

Phrased differently, the criterion allows us to witness the presence of a highly entangled state by showing that its local eigenvalues are incompatible with all less-entangled classes. Strikingly, there are always only finitely many entanglement polytopes, and they naturally form a hierarchy: if a state in the class \mathcal{C} can be approximated arbitrarily well by states from \mathcal{D} then $\Delta_{\mathcal{C}} \subseteq \Delta_{\mathcal{D}}$. This reflects geometrically the fact that states in the second class are more powerful for quantum information processing.

In order to compute $\Delta_{\mathcal{C}}$, and to see that it is indeed a convex polytope, we use tools from algebraic geometry and group representation theory, presented in detail in (14). We use the characterization of SLOCC operations as invertible local operators $A_1 \otimes \dots \otimes A_N$ (6), which act on the class \mathcal{C} , and therefore also on the set of polynomial functions on \mathcal{C} . The irreducible subspaces of this action correspond to covariants, i.e. vector-valued polynomial functions transforming in a well-defined way. By the representation theory of Lie groups, each covariant is labeled by a highest weight $\vec{\mu} = (\vec{\mu}^{(1)}, \dots, \vec{\mu}^{(N)})$, where the $\vec{\mu}^{(k)}$ are vectors of natural numbers, whose entries are ordered decreasingly and sum to the degree n of the polynomial. Thus, any normalized highest weight $\vec{\mu}/n$ formally looks like an eigenvalue vector $\vec{\lambda}$. This formal similarity corresponds to a factual correspondence: $\Delta_{\mathcal{C}}$ is essentially given by those $\vec{\mu}/n$'s whose associated covariants do not vanish on \mathcal{C} (15). The statement that $\Delta_{\mathcal{C}}$ is a convex polytope then follows from the fact that the covariants form a finitely-generated algebra (15). We explain how to algorithmically compute a finite set of generators by using computational invariant theory (16), motivated in part by (17). The polytope can then be obtained as the convex hull of the normalized highest weights $\vec{\mu}/n$ of those generators which are non-zero on the class \mathcal{C} .

In the following we illustrate our method with a number of paradigmatic examples: For qubit systems, each single-particle reduced density matrix $\rho^{(k)}$ has two eigenvalues, which are non-negative and sum to one; hence its spectrum is completely characterized by the maximal eigenvalue $\lambda_{\max}^{(k)}$, which can take values in the interval $[0.5, 1]$. In the case of three qubits, we may therefore regard the entanglement polytopes as subsets of three-dimensional space. There are two full-dimensional polytopes (18): one for the W class (the upper pyramid in Fig. 1) and the other for the GHZ class (the entire polytope, i.e., the union of both pyramids). The tip of the upper pyramid constitutes a polytope by itself, indicating a product state. Three further one-dimensional polytopes are given by the edges emanating from this vertex. They correspond to the three possibilities of embedding a Bell state into three systems. Thus, eigenvalues in the interior of the polytope are compatible only with W and GHZ classes, i.e., genuine three-partite entanglement. Likewise, if the eigenvalues lie in the lower pyramid

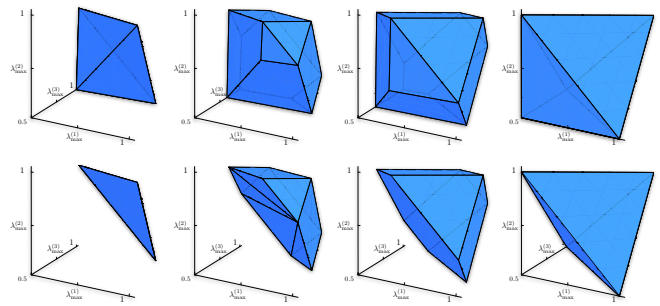


Figure 2. *Cross-sections of two entanglement polytopes for four qubits.* Each row shows cross-sections of a four-dimensional entanglement polytope for four values of $\lambda_{\max}^{(4)}$: 0.5, 0.66, 0.83 and 1. The first row corresponds to the entanglement class L_{a_4} for $a = 0$ in the characterization of (8) and the second row to the four-qubit W class—one can clearly identify the “upper-pyramid form” explained in the text. Several properties that had previously been computed algebraically (8) can be read off directly: E.g., the final column corresponds to the situation when the fourth qubit has been projected onto a pure state; as apparent from the polytopes, the state of the remaining three sites is generically of GHZ type in the first row, and of W type in the second row. See (26) for an interactive visualization of all four-qubit entanglement polytopes.

then by Eq. 1 the state cannot be contained in the closure of the W class—we have witnessed GHZ-type entanglement.

In systems of 4 qubits, there exist 9 infinite families of entanglement classes, each described by up to four complex parameters (8) that are not directly accessible; hence, a complete classification is too detailed to be practical. In contrast, the polytope method strikes an attractive balance between coarse-graining and preserving structure (Fig. 2): Up to permutations, there are 12 entanglement polytopes, 7 of which are full-dimensional and correspond to distinct types of genuine four-partite entanglement. One example is the 4-qubit W class: in complete analogy to the previous case, its polytope is an “upper pyramid” of eigenvalues that fulfill $\lambda_{\max}^{(1)} + \lambda_{\max}^{(2)} + \lambda_{\max}^{(3)} + \lambda_{\max}^{(4)} \geq 3$.

Quantum states which are genuinely multipartite entangled are of particular interest (19). These are the states which do not factorize with respect to any partition of the qubits into two sets. We show for arbitrary qubit systems that the entanglement polytopes of the biseparable states (i.e., the states that do factorize) do not account for all possible eigenvalues. Therefore, the presence of genuine multipartite entanglement in a pure quantum state can be certified by checking that the local eigenvalues do not lie in any biseparable polytope (Fig. 3).

Entanglement polytopes can also be constructed for quantum systems composed of bosons or fermions. Since the individual particles are indistinguishable, the reduced density matrices $\rho^{(k)}$ and their eigenvalues $\vec{\lambda}^{(k)}$ all coincide. In the case of qubits, the entanglement polytopes are therefore intervals describing the possible values of the maximal local eigenvalue for states in the class. For bosons, the right endpoint of the interval is always equal to one, corresponding to a coherent state, while the left endpoint $\gamma_{\mathcal{C}}$ corresponds to the most entangled states in the class. These are the symmetric Dicke states with mean spin $m \geq 0$ per particle, for which $\gamma_{\mathcal{C}} = 0.5 + m$, and they

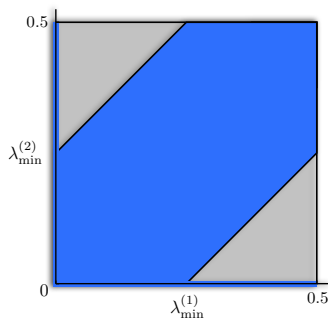


Figure 3. *Witnessing genuine multipartite entanglement.* The figure displays the two-dimensional cross-section through the six-qubit eigenvalue polytope where we fix $\lambda_{\min}^{(3)} = \dots = \lambda_{\min}^{(6)} = 0.125$. If the local eigenvalues do not belong to any biseparable entanglement polytope (blue region) then any corresponding pure state necessarily contains genuine six-qubit entanglement.

include the GHZ state for $\gamma_C = 0.5$. In (14) we also describe the entanglement polytopes for the Borland–Dennis system, which is composed of three fermions with local rank six (20).

We can also obtain quantitative information about the multipartite entanglement of a quantum state, e.g., by witnessing genuine k -partite entanglement (19) using a generalization of the argument sketched above. Furthermore, we may consider the linear entropy of entanglement $E(\psi) = 1 - \frac{1}{N} \sum_{j=1}^N \text{tr}(\rho^{(j)})^2$ used, e.g., in metrology (21). Entanglement polytopes allow us to bound the maximal linear entropy of entanglement distillable by SLOCC operations. Since $E(\psi)$ corresponds to the Euclidean length of the vector of local eigen-

values, shorter vectors imply more entanglement. In particular, quantum states of maximal entropy of entanglement in a class \mathcal{C} map to the point of minimal distance to the origin in the entanglement polytope $\Delta_{\mathcal{C}}$. Therefore, if the local eigenvalues of a given state lie only in polytopes with small distance to the origin, a high amount of entanglement can be distilled. In (14) we turn this observation into a quantitative statement and describe a distillation algorithm.

Quantum states prepared in the laboratory are always subject to noise and hence never perfectly pure. Our method for witnessing entanglement using Eq. 1 can be adapted to this situation as long as the noise is not too large. To make this statement precise, we assume that a lower bound $1 - \varepsilon$ on the purity $\text{tr} \rho^2$ of a quantum state ρ is available. This implies that ρ has fidelity $\langle \psi | \rho | \psi \rangle \geq 1 - \varepsilon$ with a pure state $|\psi\rangle$ whose local eigenvalues deviate from the measured ones by no more than a small amount $\delta(\varepsilon)$. In the case of N qubits one has that $\delta(\varepsilon) \approx N\varepsilon/2$ for small impurities. Therefore, as long as the distance of the measured eigenvalues $\vec{\lambda}$ to the entanglement polytope $\Delta_{\mathcal{C}}$ is at least $\delta(\varepsilon)$, the experimentally prepared state ρ has high fidelity with a pure state that is more entangled than the class \mathcal{C} . These ideas can be further extended to show that ρ itself cannot be written as a convex combination of quantum states in a given entanglement class, as we describe in (14). Unlike the local eigenvalues, the purity $\text{tr} \rho^2$ cannot be determined by single-particle tomography alone. However, it is in general not necessary to perform full tomography of the global state in order to estimate the purity (22). Whereas it is an experimental challenge to achieve the levels of purity necessary for the application of our method, we believe that they are in the reach of current technology (23–25).

-
- [1] G. Vidal, “Efficient Classical Simulation of Slightly Entangled Quantum Computations,” *Phys. Rev. Lett.* **91**, 147902 (2003).
- [2] D. Leibfried *et al.*, “Toward Heisenberg-Limited Spectroscopy with Multiparticle Entangled States,” *Science* **304**, 1476 (2004).
- [3] V. Giovannetti, S. Lloyd, and L. Maccone, “Quantum-Enhanced Measurements: Beating the Standard Quantum Limit,” *Science* **306**, 1330 (2004).
- [4] R. Horodecki, P. Horodecki, M. Horodecki, and K. Horodecki, “Quantum entanglement,” *Rev. Mod. Phys.* **81**, 865 (2009).
- [5] C. H. Bennett, S. Popescu, D. Rohrlich, J. A. Smolin, and A. V. Thapliyal, “Exact and asymptotic measures of multipartite pure-state entanglement,” *Phys. Rev. A* **63**, 012307 (2000).
- [6] W. Dür, G. Vidal, and J. I. Cirac, “Three qubits can be entangled in two inequivalent ways,” *Phys. Rev. A* **62**, 062314 (2000).
- [7] D. M. Greenberger, M. A. Horne, and A. Zeilinger, “Going Beyond Bell’s Theorem,” in *Bell’s Theorem, Quantum Theory, and Conceptions of the Universe* (Kluwer, 1989) p. 69.
- [8] F. Verstraete, J. Dehaene, B. De Moor, and H. Verschelde, “Four qubits can be entangled in nine different ways,” *Phys. Rev. A* **65**, 052112 (2002).
- [9] M. Christandl and G. Mitchison, “The Spectra of Quantum States and the Kronecker Coefficients of the Symmetric Group,” *Commun. Math. Phys.* **261**, 789 (2006).
- [10] A. Klyachko, “Quantum marginal problem and representations of the symmetric group,” arXiv:quant-ph/0409113 (2004).
- [11] S. Daftuar and P. Hayden, “Quantum state transformations and the Schubert calculus,” *Ann. Phys.* **315**, 80 (2004).
- [12] A. J. Coleman and V. I. Yukalov, *Reduced Density Matrices: Coulson’s Challenge* (Springer, 2000).
- [13] A. Klyachko, “Quantum marginal problem and N -representability,” *J. Phys.: Conf. Ser.* **36**, 72 (2006).
- [14] Further details can be found in the supplementary online text.
- [15] M. Brion, “Sur l’image de l’application moment,” in *Séminaire d’Algèbre P. Dubreil et M.-P. Malliavin* (Springer, 1987) p. 177.
- [16] H. Derksen and G. Kemper, *Computational Invariant Theory* (Springer, 2002).
- [17] B. Doran and F. Kirwan, “Towards non-reductive geometric invariant theory,” *Pure Appl. Math. Q.* **3**, 61 (2007).
- [18] Y.-J. Han, Y.-S. Zhang, and G.-C. Guo, “Compatible conditions, entanglement, and invariants,” *Phys. Rev. A* **70**, 042309 (2004).
- [19] O. Gühne, G. Toth, and H. J. Briegel, “Multipartite entanglement in spin chains,” *New J. Phys.* **7** (2005).
- [20] R. E. Borland and K. Dennis, “The conditions on the one-matrix for three-body fermion wavefunctions with one-rank equal to six,” *J. Phys. B* **5**, 7 (1972).
- [21] K. Furuya, M. C. Nemes, and G. Q. Pellegrino, “Quantum Dynamical Manifestation of Chaotic Behavior in the Process of Entanglement,” *Phys. Rev. Lett.* **80**, 5524 (1998).
- [22] H. Buhrman, R. Cleve, J. Watrous, and R. de Wolf, “Quantum Fingerprinting,” *Phys. Rev. Lett.* **87**, 167902 (2001).

- [23] A. Rauschenbeutel *et al.*, “Step-by-Step Engineered Multiparticle Entanglement,” *Science* **288** (2000).
- [24] J.-W. Pan, M. Daniell, S. Gasparoni, G. Weihs, and A. Zeilinger, “Experimental Demonstration of Four-Photon Entanglement and High-Fidelity Teleportation,” *Phys. Rev. Lett.* **86**, 4435 (2001).
- [25] T. Monz *et al.*, “14-Qubit Entanglement: Creation and Coherence,” *Phys. Rev. Lett.* **106**, 130506 (2011).
- [26] M. Walter, B. Doran, D. Gross, and M. Christandl, www.entanglement-polytopes.org (2012).
- [27] F. C. Kirwan, *Cohomology of quotients in symplectic and algebraic geometry* (Princeton University Press, 1984).
- [28] M. A. Nielsen and I. L. Chuang, *Quantum Computation and Quantum Information* (Cambridge University Press, 2004).
- [29] J. Eisert and D. Gross, “Multiparticle Entanglement,” in *Lectures on Quantum Information* (Wiley-VCH, 2008) p. 237.
- [30] O. Gühne and G. Toth, “Entanglement detection,” *Phys. Rep.* **474**, 1 (2009).
- [31] A. Klyachko, “Coherent states, entanglement, and geometric invariant theory,” arXiv:quant-ph/0206012 (2002).
- [32] E. Briand, J.-G. Luque, and J.-Y. Thibon, “A complete set of covariants of the four qubit system,” *J. Phys. A* **38**, 9915 (2003).
- [33] F. Verstraete, J. Dehaene, and B. De Moor, “Normal forms and entanglement measures for multipartite quantum states,” *Phys. Rev. A* **68**, 012103 (2003).
- [34] A. Miyake, “Classification of multipartite entangled states by multidimensional determinants,” *Phys. Rev. A* **67**, 012108 (2003).
- [35] M. S. Leifer, N. Linden, and A. Winter, “Measuring polynomial invariants of multiparty quantum states,” *Phys. Rev. A* **69**, 052304 (2004).
- [36] A. Osterloh and J. Siewert, “Constructing N -qubit entanglement monotones from antilinear operators,” *Phys. Rev. A* **72**, 012337 (2005).
- [37] A. Osterloh and J. Siewert, “Entanglement monotones and maximally entangled states in multipartite qubit systems,” *Int. J. Quant. Inf.* **4**, 531 (2006).
- [38] A. Klyachko, “Dynamic Symmetry Approach to Entanglement,” in *Proc. NATO Adv. Study Inst. on Physics and Theo. Comp. Sci.* (IOS Press, 2007).
- [39] D. Ž. Đoković and A. Osterloh, “On polynomial invariants of several qubits,” *J. Math. Phys.* **50**, 033509 (2009).
- [40] T. Bastin *et al.*, “Operational Families of Entanglement Classes for Symmetric N -Qubit States,” *Phys. Rev. Lett.* **103**, 070503 (2009).
- [41] A. Osterloh, “Classification of qubit entanglement: $SL(2, C)$ versus $SU(2)$ invariance,” *Appl. Phys. B* **98**, 609 (2010).
- [42] G. Gour and N. R. Wallach, “Necessary and sufficient conditions for local manipulation of multipartite pure quantum states,” *New J. Physics* **13**, 073013 (2011).
- [43] O. Viehmann, C. Eltschka, and J. Siewert, “Polynomial invariants for discrimination and classification of four-qubit entanglement,” *Phys. Rev. A* **83**, 052330 (2011).
- [44] C. Eltschka, T. Bastin, A. Osterloh, and J. Siewert, “Multipartite-entanglement monotones and polynomial invariants,” *Phys. Rev. A* **85**, 022301 (2012).
- [45] V. Guillemin and S. Sternberg, *Symplectic Techniques in Physics* (Cambridge University Press, 1984).
- [46] F. Kirwan, “Convexity properties of the moment mapping, III,” *Invent. Math.* **77**, 547 (1984).
- [47] W. Fulton, *Young Tableaux* (London Mathematical Society, 1997).
- [48] R. Hartshorne, *Algebraic Geometry* (Springer, 1977).
- [49] A. Knapp, *Lie Groups: Beyond an Introduction*, 2nd ed. (Birkhäuser, 2002).
- [50] H. Kraft, *Geometrische Methoden in der Invariantentheorie* (Vieweg, 1985).
- [51] F. D. Grosshans, *Algebraic homogeneous spaces and invariant theory* (Springer-Verlag, 1997).
- [52] I. Dolgachev, *Lectures on Invariant Theory* (Cambridge University Press, 2003).
- [53] M. Christandl, B. Doran, S. Kousidis, and M. Walter, “Eigenvalue Distributions of Reduced Density Matrices,” arXiv:1204.0741 (2012).
- [54] A. Higuchi, A. Sudbery, and J. Szulc, “One-qubit reduced states of a pure many-qubit state: polygon inequalities,” *Phys. Rev. Lett.* **90**, 107902 (2003).
- [55] N. Linden, S. Popescu, and W. K. Wootters, “Almost Every Pure State of Three Qubits Is Completely Determined by Its Two-Particle Reduced Density Matrices,” *Phys. Rev. Lett.* **89**, 207901 (2002).
- [56] L. E. Würflinger, J.-D. Bancal, A. Acín, N. Gisin, and T. Vértesi, “Nonlocal multipartite correlations from local marginal probabilities,” *Phys. Rev. A* **86**, 032117 (2012).
- [57] K. M. R. Audenaert, “Subadditivity of q -entropies for $q > 1$,” *J. Math. Phys.* **48**, 083507 (2007).
- [58] C. A. Fuchs and J. van de Graaf, “Cryptographic distinguishability measures for quantum-mechanical states,” *IEEE Trans. Inf. Theory* **45**, 1216 (1999).
- [59] G. Kempf and L. Ness, “The length of vectors in representation spaces,” in *Algebraic geometry* (Springer, 1979) p. 233.
- [60] D. Mumford, J. Fogarty, and F. Kirwan, *Geometric Invariant Theory*, third enlarged ed. (Springer, 1994).
- [61] W. H. Zurek, S. Habib, and J. P. Paz, “Coherent states via decoherence,” *Phys. Rev. Lett.* **70**, 1187 (1993).
- [62] H. Barnum, E. Knill, G. Ortiz, R. Somma, and L. Viola, “A Subsystem-Independent Generalization of Entanglement,” *Phys. Rev. Lett.* **92**, 107902 (2004).
- [63] S. Boixo and A. Monras, “Operational Interpretation for Global Multipartite Entanglement,” *Phys. Rev. Lett.* **100**, 100503 (2008).
- [64] D. A. Meyer and N. R. Wallach, “Global entanglement in multiparticle systems,” *J. Math. Phys.* **43**, 4273 (2002).
- [65] G. K. Brennen, “An observable measure of entanglement for pure states of multi-qubit systems,” *Quant. Inf. and Comp.* **3**, 619 (2003).
- [66] S. Hill and W. K. Wootters, “Entanglement of a Pair of Quantum Bits,” *Phys. Rev. Lett.* **78**, 5022 (1997).
- [67] P. J. Olver, *Classical Invariant Theory* (Cambridge University Press, 1999).
- [68] J.-G. Luque, *Invariants des hypermatrices*, Habilitation (2007).
- [69] A. Sawicki, M. Walter, and M. Kuš, “When is a pure state of three qubits determined by its single-particle reduced density matrices?” *J. Phys. A* **46**, 055304 (2013).
- [70] C. Le Paige, “Sur les formes trilineaires,” *C. R. Acad. Sci. Paris* **92**, 1103 (1881).
- [71] H. J. Briegel and R. Raussendorf, “Persistent entanglement in arrays of interacting particles,” *Phys. Rev. Lett.* **86**, 910 (2001).
- [72] M. Horodecki, P. Horodecki, and R. Horodecki, “Separability of n -particle mixed states: necessary and sufficient conditions in terms of linear maps,” *Phys. Lett. A* **283**, 1 (2001).
- [73] F. Levi and F. Mintert, “Hierarchies of Multipartite Entanglement,” *Phys. Rev. Lett.* **110**, 150402 (2013).
- [74] M. Seevinck and J. Uffink, “Sufficient conditions for three-particle entanglement and their tests in recent experiments,” *Phys. Rev. A* **65**, 012107 (2001).
- [75] M. Huber, F. Mintert, A. Gabriel, and B. C. Hiesmayr, “Detection of high-dimensional genuine multipartite entanglement of mixed states,” *Phys. Rev. Lett.* **104**, 210501 (2010).

- [76] P. Mathonet, S. Krins, M. Godefroid, L. Lamata, E. Solano, and T. Bastin, “Entanglement equivalence of N -qubit symmetric states,” *Phys. Rev. A* **81**, 052315 (2010).
- [77] J. P. S. Kung and G.-C. Rota, “The invariant theory of binary forms,” *Bull. Amer. Math. Soc.* **10**, 27 (1984).
- [78] R. H. Dicke, “Coherence in spontaneous radiation processes,” *Phys. Rev.* **93**, 99 (1954).
- [79] P. Lévy and P. Vrana, “Three fermions with six single particle states can be entangled in two inequivalent ways,” *Phys. Rev. A* **78**, 022329 (2008).
- [80] J. A. Schouten, “Klassifizierung der alternierenden Größen dritten Grades in 7 Dimensionen,” *Rend. Circ. Mat. Palermo* **55**, 137 (1931).
- [81] R. Ehrenborg, “Canonical Forms of Two by Two by Two Matrices,” *J. Alg.* **213**, 195 (1999).
- [82] V. Coffman, J. Kundu, and W. K. Wothers, “Distributed entanglement,” *Phys. Rev. A* **61**, 052306 (2000).
- [83] O. Chterental and D. Ž. Đoković, “Normal forms and tensor ranks of pure states of four qubits,” in *Linear Algebra Research Advances* (Nova Science Publishers, Inc., 2007) pp. 133–167.

Acknowledgements: We thank A. Botero, F. Brandão, P. Bürgisser, C. Ikenmeyer, F. Kirwan, F. Mintert, G. Mitchison, A. Osterloh, and P. Vrana for valuable discussions. This work is supported by the German Science Foundation (grant CH 843/2–1), the Swiss National Science Foundation (grants PP00P2_128455, 20CH21_138799 (CHIST-ERA project QQC) and 200021_138071), the Swiss National Center of Competence in Research ‘QSIT’, and the Excellence Initiative of the German Federal and State Governments (grant ZUK 43). After completion of this work, we have learned about independent related work by Sawicki, Ozmaniec and Kuś.

Supplementary Materials:

www.sciencemag.org/content/340/6137/1205/suppl/DC1

Supplementary Text

Figs. S1–S4

Tables S1–S3

References (27–83)

SUPPLEMENTARY TEXT

1. Introduction

In this supplement, we will give rigorous proofs of the main properties of entanglement polytopes (§ 3) and describe an algorithmic method for their computation, which we illustrate with several worked examples (§ 5). Moreover, we elaborate on the properties of the linear entropy of entanglement and derive the gradient flow procedure for entanglement distillation that has been sketched in the main body of the article (§ 4). Our main technical tools are Brion’s invariant-theoretic description of moment polytopes (15) seen through the lens of non-reductive group actions (17), and Kirwan’s analysis of the equivariant Morse gradient flow for the norm square of a moment map (27).

For clarity of exposition, we will describe our results for a system composed of N distinguishable subsystems with d_k degrees of freedom, respectively, and Hilbert space

$$\mathcal{H} = \mathbb{C}^{d_1} \otimes \dots \otimes \mathbb{C}^{d_N}.$$

In the context of multi-particle entanglement, we will think of each of the N subsystems as corresponding to an individual particle. However, the subsystems can be of more general nature and, e.g., describe different degrees of freedom such as position and spin. All results can be adapted to systems composed of bosons or fermions by replacing \mathcal{H} with the (anti)symmetric subspace (§ 5). We shall denote by

$$\mathbb{P}(\mathcal{H}) = \{\rho = |\psi\rangle\langle\psi| : \langle\psi|\psi\rangle = 1\}$$

the projective space of *pure states*; the expectation value of an observable O in a pure state ρ is given by $\text{tr}(\rho O) = \langle\psi|O|\psi\rangle$. The effective state of the k -th particle is described by the (*one-body*) *reduced density matrix* $\rho^{(k)}$, which by definition reproduces the expectation values of all one-body observables $O^{(k)}$,

$$\text{tr}(\rho^{(k)} O^{(k)}) = \text{tr}(\rho (\mathbb{1}^{\otimes(k-1)} \otimes O^{(k)} \otimes \mathbb{1}^{\otimes(N-k)})) = \langle\psi|\mathbb{1}^{\otimes(k-1)} \otimes O^{(k)} \otimes \mathbb{1}^{\otimes(N-k)}|\psi\rangle \quad (\text{S1})$$

The one-body reduced density matrices $\rho^{(k)}$ are in general *mixed states*, i.e., convex mixtures of pure states. Formally, they are positive semidefinite Hermitian operators of trace one. By the spectral theorem, each $\rho^{(k)}$ can be diagonalized, and the *local eigenvalues* $\vec{\lambda}^{(k)} = \vec{\lambda}(\rho^{(k)})$ are vectors of non-negative numbers summing to one (which we assume by convention to be weakly decreasing).

2. Multi-Particle Entanglement and Stochastic Local Operations and Classical Communication (SLOCC)

A pure quantum state $\rho = |\psi\rangle\langle\psi|$ of a multi-particle system is called *entangled* if it cannot be written as a tensor product (28)

$$|\psi\rangle \neq |\psi^{(1)}\rangle \otimes \dots \otimes |\psi^{(N)}\rangle.$$

It is easy to see that ρ is unentangled, or *separable*, if and only if all its one-body reduced density matrices $\rho^{(k)}$ are pure states, that is, if and only if $\vec{\lambda}^{(k)} = (1, 0, \dots, 0)$ for $k = 1, \dots, N$.

In order to classify the entanglement present in a given multipartite quantum state ρ , it is useful to compare its capability for quantum information processing tasks with that of other quantum states. Specifically, we shall think of ρ to be at least as entangled as any other quantum state ρ' that can be produced from a single copy of ρ by performing a sequence of *stochastic local operations* (i.e., local operations which succeed with some positive probability, e.g., by post-selecting on a certain measurement outcome) and *classical communication* (SLOCC) (5, 6). If, conversely, ρ can also be produced from ρ' then we can think of the two states as possessing the same kind of multi-particle entanglement. In this way the set of quantum states is partitioned into equivalence classes. For pure states $\rho = |\psi\rangle\langle\psi|$ and $\rho' = |\psi'\rangle\langle\psi'|$, it has been shown that they are equivalent under SLOCC if and only if there exist invertible operators $A^{(k)}$ such that

$$|\psi'\rangle = (A^{(1)} \otimes \dots \otimes A^{(N)}) |\psi\rangle.$$

Indeed, the operators $A^{(k)}$ can be defined by following a successful branch of a conversion protocol. Conversely, given operators $A^{(k)}$ it suffices to perform successive local POVM measurements with Kraus operators

$$S^{(k)} = \sqrt{p^{(k)}} A^{(k)}, \quad F^{(k)} = \sqrt{\mathbb{1} - p^{(k)}} (A^{(k)})^\dagger A^{(k)}, \quad (\text{S2})$$

where $p^{(k)}$ is a suitable normalization constant. If all measurements succeed (outcomes $S^{(1)}, \dots, S^{(k)}$) then ρ' has been successfully distilled from ρ (6). Mathematically, it is convenient to define an action of the Lie group $G = \text{SL}(d_1) \times \dots \times \text{SL}(d_N)$ of invertible local operators of determinant one on the projective space $\mathbb{P}(\mathcal{H})$ by

$$g \cdot |\psi\rangle\langle\psi| := \frac{(g^{(1)} \otimes \dots \otimes g^{(N)})|\psi\rangle\langle\psi|(g^{(1)} \otimes \dots \otimes g^{(N)})^\dagger}{\|(g^{(1)} \otimes \dots \otimes g^{(N)})|\psi\rangle\|^2}, \quad (\text{S3})$$

where $g = (g^{(1)}, \dots, g^{(N)}) \in G$. Then the result of (6) states that two pure states ρ and ρ' are equivalent under SLOCC if and only if $G \cdot \rho = G \cdot \rho'$. In other words, the *SLOCC entanglement class* containing ρ is just the orbit $\mathcal{C} = G \cdot \rho$. Clearly, the unentangled states form a single SLOCC class.

The closure $\overline{\mathcal{C}} = \overline{G \cdot \rho}$ of an entanglement class contains in addition those quantum states which can be arbitrarily well approximated by a state in the class. In this way, the closure of an entanglement class can be given a similar operational interpretation as the class itself. While the entanglement classes partition the set of multi-particle quantum states, their closures naturally form a hierarchy. This is because they are stable under SLOCC operations; indeed, it is immediate that $\rho' \in \overline{G \cdot \rho}$ implies $\overline{G \cdot \rho'} \subseteq \overline{G \cdot \rho}$. In particular, every entanglement class contains in its closure the class of unentangled states.

In summary, stochastic local operations and classical communication provide a systematic way of studying multi-particle entanglement. However, it is immediate from the fact that the dimension of G grows only linearly with N that there is generically an infinite number of distinct SLOCC entanglement classes labeled by an exponential number of continuous parameters (cf. § 5). It is therefore necessary to coarsen the classification in a systematic way in order to arrive at a tractable way of witnessing multi-particle entanglement.

We note that an extraordinary amount of research has been devoted to the task of classifying SLOCC entanglement and identifying it experimentally. The field is far too large to allow for an exhaustive bibliography. For reviews on the general theory, see (4, 29); a review focussing on detection is (30). Methods from algebraic geometry and classical invariant theory have long been used to analyze entanglement classes, see, e.g., (8, 18, 31–44) and references therein.

3. Entanglement Polytopes

a. Definition

The *entanglement polytope* of an entanglement class \mathcal{C} is by definition

$$\Delta_{\mathcal{C}} = \left\{ (\vec{\lambda}^{(1)}, \dots, \vec{\lambda}^{(N)}) : \vec{\lambda}^{(k)} = \vec{\lambda}(\rho^{(k)}), \rho \in \overline{\mathcal{C}} \right\},$$

the set of tuples of local eigenvalues of the quantum states in the closure of the entanglement class. We will show below that this set is in fact a convex polytope. The set of entanglement polytopes forms a hierarchy which coarsens the hierarchy of the closures of entanglement classes described above. Namely,

$$\overline{\mathcal{C}} \subseteq \overline{\mathcal{D}} \implies \Delta_{\mathcal{C}} \subseteq \Delta_{\mathcal{D}}.$$

In particular, if a pure quantum state $\rho = |\psi\rangle\langle\psi|$ is contained in an entanglement class \mathcal{C} then its collection of local eigenvalues is contained in the corresponding entanglement polytope $\Delta_{\mathcal{C}}$. That is,

$$\rho \in \mathcal{C} \implies (\vec{\lambda}^{(1)}, \dots, \vec{\lambda}^{(N)}) \in \Delta_{\mathcal{C}}.$$

Equivalently, if the collection of local eigenvalues is not contained in the entanglement polytope then the quantum state is necessarily in a different entanglement class:

$$(\vec{\lambda}^{(1)}, \dots, \vec{\lambda}^{(N)}) \notin \Delta_{\mathcal{C}} \implies \rho \notin \mathcal{C} \quad (\text{S4})$$

This establishes our main criterion for witnessing multi-particle entanglement.

b. Invariant-Theoretic Description

In order to analyze the properties of entanglement polytopes, it is useful to introduce the map

$$\Phi: \rho = |\psi\rangle\langle\psi| \mapsto (\rho^{(1)}, \dots, \rho^{(N)})$$

which assigns to a quantum state the collection of its one-body reduced density matrices. Given a product of local unitaries $U = U^{(1)} \otimes \dots \otimes U^{(N)}$, it follows from (S1) that

$$\Phi(U\rho U^\dagger) = (U^{(1)}\rho^{(1)}(U^{(1)})^\dagger, \dots, U^{(N)}\rho^{(N)}(U^{(N)})^\dagger). \quad (\text{S5})$$

We can therefore jointly diagonalize the reduced density matrices by applying suitable local unitaries. On the other hand, we observe that the action $\rho \mapsto U\rho U^\dagger$ is simply the restriction of (S3) to the subgroup of local unitaries $K = \text{SU}(d_1) \times \dots \times \text{SU}(d_N)$ of the group $G = \text{SL}(d_1) \times \dots \times \text{SL}(d_N)$ introduced in § 2 (the denominator is equal to unity since any unitary is norm-preserving), so that the entanglement class is left unchanged. We conclude that for every quantum state $\rho \in \mathcal{C}$ there exists a quantum state ρ' in the same entanglement class whose reduced density matrices are diagonal in the computational basis. As we may identify diagonal density matrices with their collection of eigenvalues (for definiteness, we shall require the diagonal entries to be arranged in weakly decreasing order), each entanglement polytope can be written as an intersection

$$\Delta_{\mathcal{C}} = \Phi(\overline{\mathcal{C}}) \cap D_{\downarrow}, \quad (\text{S6})$$

where we denote by D_{\downarrow} the set of tuples of diagonal density matrices with weakly decreasing entries.

In mathematical terms, the map Φ can be identified with the canonical *moment map* for the action of K on the projective space $\mathbb{P}(\mathcal{H})$ (27, 45). Indeed, by (S5) it is equivariant with respect to the action of K on tuples of reduced density matrices, which can be identified with the coadjoint action of K on the dual of its Lie algebra, and its components are Hamiltonian functions with respect to the Fubini–Study symplectic form ω_{FS} ,

$$d\langle \Phi, X \rangle (i\widehat{Y}_\rho) = i \text{tr}([Y, \rho]X) = i \text{tr}(\rho[X, Y]) = \omega_{\text{FS}}(i\widehat{X}_\rho, i\widehat{Y}_\rho), \quad (\text{S7})$$

where X and Y are Hermitian operators on \mathcal{H} and where $\widehat{Z}_\rho = \left. \frac{d}{dt} \right|_{t=0} e^{tZ} \cdot \rho = \left. \frac{d}{dt} \right|_{t=0} e^{tZ} |\psi\rangle\langle\psi| e^{tZ^\dagger} / \|e^{tZ} |\psi\rangle\|_2^2$ is the tangent vector generated by the infinitesimal action of an arbitrary operator Z ; in particular, $i\widehat{X}_\rho = i[X, \rho]$ and $\widehat{X}_\rho = \{X, \rho\} - 2 \text{tr}(\rho X)\rho$. Formally, the above equation should be restricted to local observables X of trace zero, since only these correspond to elements in the Lie algebra of the group K .

It follows that (S6) is just the definition of the *moment polytope*, or *Kirwan polytope*, for the subvariety $\overline{\mathcal{C}} \subseteq \mathbb{P}(\mathcal{H})$, with D_{\downarrow} corresponding to a choice of positive Weyl chamber. It is a celebrated result in mathematics that the moment polytope of a compact symplectic manifold is a convex polytope (46). For the singular case of G -stable irreducible projective subvarieties of projective spaces, which is a category of spaces that includes the closures of any entanglement class, this has been established by Brion (15).

Brion’s proof of convexity relies on an alternative, invariant-theoretic description of the moment polytopes. In order to apply his results to the case of entanglement polytopes, we need some notions from representation theory and invariant theory. Recall that the finite-dimensional polynomial irreducible representations of the group $\text{GL}(d)$ of invertible $d \times d$ -matrices are labeled by integer vectors $\vec{\mu} \in \mathbb{Z}_{\geq 0}^d$ with weakly decreasing entries—their highest weight, or Young diagram (47). The irreducible representations of $\text{SL}(d)$ can be obtained by restriction, and they will be denoted by $V_{\vec{\mu}}^d$. Finally, a *covariant* of degree n and weights $\vec{\mu}^{(1)}, \dots, \vec{\mu}^{(N)}$ is by definition a G -equivariant map

$$\mathcal{H} = \mathbb{C}^{d_1} \otimes \dots \otimes \mathbb{C}^{d_N} \longrightarrow V_{\vec{\mu}^{(1)}}^{d_1} \otimes \dots \otimes V_{\vec{\mu}^{(N)}}^{d_N}$$

whose components are homogeneous polynomials of degree n . Note that the right-hand side is a G -representation in the obvious way. We shall require each $\vec{\mu}^{(k)}$ to satisfy $\sum_j \mu_j^{(k)} = n$; this can always be satisfied and does not impose an additional restriction. Moreover, we observe that even though covariants are defined on the Hilbert space \mathcal{H} , their non-vanishing can be well-defined on subsets of the projective space $\mathbb{P}(\mathcal{H})$ by taking any representative vector, since they are homogeneous functions; we will do so without further mention. We can now specialize the main result of (15) to our setting:

Theorem 1. *The entanglement polytope of an entanglement class $\mathcal{C} = G \cdot \rho$ is equal to*

$$\Delta_{\mathcal{C}} = \overline{\left\{ \frac{1}{n} (\vec{\mu}^{(1)}, \dots, \vec{\mu}^{(N)}) : \exists a \text{ covariant of degree } n \text{ and weights } \vec{\mu}^{(k)} \text{ which is non-zero at } \rho \right\}}$$

Proof. By the above discussion and (S6), we have seen that $\Delta_{\mathcal{C}}$ is equal to the moment polytope of the G -orbit closure $\overline{\mathcal{C}}$. In (15) it is shown that this moment polytope can be described as the closure of the set of points $(\vec{\mu}^{(1)}, \dots, \vec{\mu}^{(N)})/n$ for which there exists a non-zero G -equivariant morphism

$$\varphi: \widetilde{\mathcal{C}} \rightarrow V_{\vec{\mu}^{(1)}}^{d_1} \otimes \dots \otimes V_{\vec{\mu}^{(N)}}^{d_N}$$

which is homogeneous of degree n (i.e., whose components are homogeneous polynomial functions of degree n). Here, we denote by $\widetilde{\mathcal{C}} = \{|\psi\rangle : |\psi\rangle\langle\psi| / \langle\psi|\psi\rangle \in \overline{\mathcal{C}}\}$ the affine cone over $\overline{\mathcal{C}}$. Evidently, every covariant which is non-zero at ρ restricts to a map on

$\tilde{\mathcal{C}}$ which does not vanish completely; this shows one inclusion. For the converse, we first observe that every non-zero map φ as above is automatically non-zero at ρ , for it is G -equivariant and the affine cone over $\mathcal{C} = G \cdot \rho$ is an open subset of $\tilde{\mathcal{C}}$. It remains to show that it can be extended to a G -equivariant map on all of \mathcal{H} . This can be seen as follows by using some basic algebraic geometry and representation theory (48, 49):

Since the map φ is G -equivariant and its range an irreducible representation, it is completely equivalent to consider instead of φ its component $\phi = \langle \varphi, v \rangle$ evaluated at a highest weight vector v with respect to some maximal unipotent subgroup $U \subset G$. The function ϕ is a U -invariant homogeneous polynomial function of degree n , i.e., a U -invariant element of the degree- n piece of the homogeneous coordinate ring

$$\mathbb{C}[\tilde{\mathcal{C}}]_n = \mathbb{C}[\mathcal{H}]_n / I_n,$$

where $\mathbb{C}[\mathcal{H}]$ denotes the algebra of polynomial functions on \mathcal{H} , $\mathbb{C}[\mathcal{H}]_n$ the subspace of homogeneous functions of degree n , and $I_n = \{p \in \mathbb{C}[\mathcal{H}]_n : p(\tilde{\mathcal{C}}) = 0\}$ the corresponding part of the vanishing ideal of $\tilde{\mathcal{C}}$. By averaging over the maximal compact subgroup $K \subseteq G$, we can find an orthogonal complement I_n^\perp to I_n that is G -invariant (this is oftentimes called Weyl's unitary trick). Therefore, the natural map

$$I_n^\perp \subseteq \mathbb{C}[\mathcal{H}]_n \rightarrow \mathbb{C}[\tilde{\mathcal{C}}]_n$$

is a G -isomorphism, and it can be used to find a U -invariant extension of ϕ to all of \mathcal{H} . By reversing the above procedure, we obtain a corresponding covariant which G -equivariantly extends φ to all of \mathcal{H} . \square

c. Properties and Computation

The set of covariants of fixed degree and weight form a vector space. Moreover, given any two covariants P, Q of degree n, m and weights $\vec{\mu}^{(k)}, \vec{\nu}^{(k)}$, we can form their product by defining

$$(P \circ Q)(|\psi\rangle) = (\pi^{(1)} \otimes \dots \otimes \pi^{(N)}) (P(|\psi\rangle) \otimes Q(|\psi\rangle)). \quad (\text{S8})$$

where $\pi^{(k)}: V_{\vec{\mu}^{(k)}}^{d_k} \otimes V_{\vec{\nu}^{(k)}}^{d_k} \rightarrow V_{\vec{\mu}^{(k)} + \vec{\nu}^{(k)}}^{d_k}$ denotes the projection onto the unique irreducible representation in the tensor product of two irreducible representations whose highest weight is the sum of the highest weights of the factors. The function $P \circ Q$ is a covariant of degree $n + m$ and weights $\vec{\mu}^{(k)} + \vec{\nu}^{(k)}$. Note that the point corresponding to $P \circ Q$,

$$\frac{1}{n+m} \left(\vec{\mu}^{(1)} + \vec{\nu}^{(1)}, \dots, \vec{\mu}^{(N)} + \vec{\nu}^{(N)} \right) = \frac{n}{n+m} \left(\frac{1}{n} \left(\vec{\mu}^{(1)}, \dots, \vec{\mu}^{(N)} \right) \right) + \frac{m}{n+m} \left(\frac{1}{m} \left(\vec{\nu}^{(1)}, \dots, \vec{\nu}^{(N)} \right) \right), \quad (\text{S9})$$

is a convex combination of the points corresponding to the covariants P and Q . It follows that the entanglement polytopes are convex (replace P and Q by their respective powers). If we allow for formal linear combinations of covariants of different degree or weight, we thus obtain a graded algebra, and it is well-known that this algebra is *finitely generated*, i.e., there exist finitely many covariants P_1, \dots, P_m such that any other covariant can be expressed as a linear combination of monomials in the P_j . In the literature, this is typically phrased as the well-known statement that the algebra $\mathbb{C}[\mathcal{H}]^U$ of U -invariant polynomials is finitely generated (50, 51); (S8) then corresponds to the ordinary multiplication of functions. As noted in (15), finite generation implies that moment polytopes are compact convex polytopes. Using Theorem 1, we can slightly sharpen this result for the case of entanglement polytopes:

Theorem 2. *The entanglement polytope of an entanglement class $\mathcal{C} = G \cdot \rho$ is given by the convex hull*

$$\Delta_{\mathcal{C}} = \text{conv} \left\{ \frac{1}{n_j} \left(\vec{\mu}_j^{(1)}, \dots, \vec{\mu}_j^{(N)} \right) : P_j(\rho) \neq 0 \right\},$$

where we denote by n_j the degree and by $\vec{\mu}_j^{(k)}$ the weights of a generator P_j ($j = 1, \dots, m$). In particular, $\Delta_{\mathcal{C}}$ is a compact convex polytope.

Proof. Consider a monomial $P_{j_1} \circ \dots \circ P_{j_l}$ which does not vanish on ρ . Its degree is $n = \sum_i n_{j_i}$ and its weights are given by $\vec{\mu}^{(k)} = \sum_i \vec{\mu}_{j_i}^{(k)}$. Since necessarily $P_{j_i}(\rho) \neq 0$ for all $i = 1, \dots, l$, the corresponding point

$$\frac{1}{n} \left(\vec{\mu}_j^{(1)}, \dots, \vec{\mu}_j^{(N)} \right) = \sum_i \frac{n_{j_i}}{n} \left(\frac{1}{n_{j_i}} \left(\vec{\mu}_{j_i}^{(1)}, \dots, \vec{\mu}_{j_i}^{(N)} \right) \right)$$

is contained in the convex hull displayed in the statement of the corollary.

If P is an arbitrary covariant of degree n and weights $\vec{\mu}^{(k)}$ which does not vanish on ρ , we can write it as a linear combination of monomials. If the linear combination is chosen minimally then every monomial has the same degree and weights as P . Since at least one of the monomials must not vanish on ρ , the claim follows from what we have proved above. \square

By virtue of Theorem 2, the *computation* of entanglement polytopes is a finite problem that can be completely algorithmized. Indeed, by using the relation (52, §4.2) (cf. (17))

$$\mathbb{C}[\mathcal{H}]^U \cong \left(\mathbb{C}[\mathcal{H}] \otimes \mathbb{C}[\overline{G/U}] \right)^G \cong \mathbb{C}[\mathcal{H} \times \overline{G/U}]^G$$

the problem of computing a set of generating covariants P_1, \dots, P_m is transformed into a problem of computing invariants for a complex reductive group, for which there exist algorithms in computational invariant theory (16). Once a set of generators has been found, Theorem 2 can be used to compute the entanglement polytope both for specific states as well as for families of states. We use this method to compute all examples in § 5.

Finite generation also implies other desirable properties. It is clear that there are only *finitely many* entanglement polytopes, since by Theorem 2 any entanglement polytope is the convex hull of some subset of the finite set of points

$$\mathcal{P} = \{(\vec{\mu}_j^{(1)}, \dots, \vec{\mu}_j^{(N)})/n_j : j = 1, \dots, m\}$$

Moreover, as similarly observed in (15), the set of quantum states for which all generators are non-zero,

$$\bigcap_{j=1}^m \{\rho \in \mathbb{P}(\mathcal{H}) : P_j(\rho) \neq 0\},$$

is a finite intersection of Zariski-open sets, hence itself Zariski-open. It follows that the entanglement polytope of a generic quantum state is maximal, i.e., equal to the convex hull of the finite set \mathcal{P} .

Let us briefly digress to discuss this generic entanglement polytope, which we shall denote by Δ . Clearly,

$$\begin{aligned} \Delta &= \text{conv} \left\{ \frac{1}{n_j} \left(\vec{\mu}_j^{(1)}, \dots, \vec{\mu}_j^{(N)} \right) \right\} \\ &= \overline{\left\{ \frac{1}{n} \left(\vec{\mu}^{(1)}, \dots, \vec{\mu}^{(N)} \right) : \exists \text{ a covariant of degree } n \text{ and weights } \vec{\mu}^{(k)} \right\}} \\ &= \Phi(\mathbb{P}(\mathcal{H})) \cap D_{\downarrow} \\ &= \left\{ (\vec{\lambda}^{(1)}, \dots, \vec{\lambda}^{(N)}) : \vec{\lambda}^{(k)} = \vec{\lambda}(\rho^{(k)}), \rho \in \mathbb{P}(\mathcal{H}) \right\}, \end{aligned}$$

the set of possible local eigenvalues of an arbitrary pure quantum state (not restricted to any particular entanglement class). The problem of computing this polytope is known as the *one-body quantum marginal problem* in quantum information theory and as the one-body N -representability problem in quantum chemistry (12). Its convexity has been noted in (9–11), and it has been solved by combining the invariant-theoretic characterization of Δ with some Schubert calculus and geometric invariant theory (10, 11, 13); see also (53) for a different approach relying solely on symplectic geometry. In the case of N qubits, a complete solution has been obtained in (54). More generally, the way in which properties of the global state manifest in local correlations has also been studied in the literature (55, 56).

As remarked above, convexity and invariant-theoretic descriptions can be established for arbitrary G -stable irreducible subvarieties $X \subseteq \mathbb{P}(\mathcal{H})$, not only for orbit closures (15). For instance, we may choose X to be a *Segré variety*, i.e., the set of states which are biseparable with respect to a fixed bipartition of the N subsystems (see § 5 c below for an example).

d. Experimental Noise

A quantum state prepared in the laboratory will always be a mixed state ρ and it is a priori unclear what statements can be inferred about its entanglement from its local eigenvalues. Here, we give two slightly different ways for leveraging the results discussed for pure states to the more realistic scenario of small noise.

For both approaches, we will assume that a lower bound p on the purity $\text{tr } \rho^2$ is available. One natural way of obtaining such an estimate is the well-known swap test (22) which directly estimates $\text{tr } \rho^2$ using two-particle measurements on two copies of ρ . We sketch an alternative procedure which may be simpler to implement in some platforms. It is rigorous up to an assumption on the prevailing noise mechanism: namely that it does not increase purity. This does hold, e.g., for dephasing and depolarizing noise—two models applicable to the majority of experiments. Now suppose that ρ has been prepared by acting on an initial product state with a quantum operation Λ approximating an entangling unitary gate U (e.g., a spin squeezing operation). Let Λ' be a channel approximating U^{-1} , and $\rho' = \Lambda'(\rho)$. Under said assumption, we have that $\text{tr } \rho'^2 \leq \text{tr } \rho^2$, i.e., the purity has decreased under the noisy “disentangling operation” Λ' . But ρ' is still approximately a product, so that the lower bound (57)

$$\text{tr } \rho^2 \geq \text{tr } \rho'^2 \geq \sum_{k=1}^N \|\vec{\lambda}^{(k)}(\rho')\|_2^2 - (N - 1) = p$$

for the global purity in terms of the local eigenvalue spectra is likely not to be too loose (it is tight for product states). The following bounds will produce non-vacuous results only if the purity p exceeds $1/2$, which will from now on be assumed.

The first way of dealing with noise is to realize that there is a pure state $|\psi\rangle$ with fidelity $\langle\psi|\rho|\psi\rangle \geq p$ whose vector of local eigenvalues differs from the vector of local eigenvalues of ρ by at most $N(1 - \sqrt{2p-1})$.

To see this, expand the mixed state ρ in its eigenbasis $\rho = \sum_i r_i |\psi_i\rangle\langle\psi_i|$ with eigenvalues ordered non-increasingly, $r_i \geq r_{i+1}$. Our assumption $p > 1/2$ on the purity implies immediately that the maximal eigenvalue is also lower-bounded by $1/2$,

$$r_1 = r_1 \sum_i r_i \geq \sum_i r_i^2 = \text{tr } \rho^2 = p > \frac{1}{2}. \quad (\text{S10})$$

On the other hand, using that $r_j \leq \sum_{i>1} r_i = 1 - r_1$ for all $j > 1$, we find that

$$p = \text{tr } \rho^2 = r_1^2 + \sum_{i>1} r_i^2 \leq r_1^2 + (1 - r_1)^2 = 1 - 2r_1(1 - r_1).$$

We solve the quadratic relation and obtain two possible solutions,

$$r_1 \leq \frac{1}{2} \left(1 - \sqrt{2p-1}\right), \quad r_1 \geq \frac{1}{2} \left(1 + \sqrt{2p-1}\right).$$

Only the right-hand side solution is compatible with $r_1 > 1/2$. From now on we will employ the convention that $\|-\|_p$, when applied to matrices, denotes the (Schatten) p -norm (in particular: $\|-\|_1$ is the trace norm). Set $|\psi\rangle := |\psi_1\rangle$. Then clearly, $\langle\psi|\rho|\psi\rangle = r_1 \geq p$ by (S10). On the other hand, by using a version of Weyl's perturbation theorem for the 1-norm (28, (11.46)), the vector of local eigenvalues only changes by

$$\sum_{k=1}^N \|\vec{\lambda}^{(k)}(\rho) - \vec{\lambda}^{(k)}(|\psi\rangle)\|_1 \leq N \|\rho - |\psi\rangle\langle\psi|\|_1 = 2N(1 - r_1) \leq N \left(1 - \sqrt{2p-1}\right). \quad (\text{S11})$$

For the case of N qubits, a further improvement can be made. Here, we are only concerned with the largest eigenvalue in each system. Due to normalization $\lambda_{\max}^{(k)} + \lambda_{\min}^{(k)} = 1$, every deviation in the maximum eigenvalue has to be accompanied by a deviation of equal magnitude of the minimum eigenvalue. Thus, the 1-norm difference of the maximum eigenvalues is exactly half the quantity estimated above:

$$\sum_k |\lambda_{\max}^{(k)}(\rho) - \lambda_{\max}^{(k)}(|\psi\rangle)| = \sum_k \frac{1}{2} \|\vec{\lambda}^{(k)}(\rho) - \vec{\lambda}^{(k)}(|\psi\rangle)\|_1 \leq \frac{N}{2} \left(1 - \sqrt{2p-1}\right). \quad (\text{S12})$$

For small noise, $p = 1 - \varepsilon \approx 1$, the right-hand side is given by $N\varepsilon/2$ to first order in ε .

We now illustrate this approach with a numerical example. Suppose that ρ is an experimentally prepared quantum state of four qubits with purity $p = 0.9$. Then by the above there exists a pure state $|\psi\rangle$ with fidelity $\langle\psi|\rho|\psi\rangle \geq 0.9$ for which (S12) reads

$$\sum_k |\lambda_{\max}^{(k)}(\rho) - \lambda_{\max}^{(k)}(|\psi\rangle)| \leq \frac{4}{2} \left(1 - \sqrt{2p-1}\right) \approx 0.21. \quad (\text{S13})$$

At this resolution, the differences between the various four-qubit entanglement polytopes are already well visible. For concreteness, suppose that we would like to use the inequality

$$\lambda_{\max}^{(1)}(|\psi\rangle) + \lambda_{\max}^{(2)}(|\psi\rangle) + \lambda_{\max}^{(3)}(|\psi\rangle) + \lambda_{\max}^{(4)}(|\psi\rangle) < 3$$

to deduce that $|\psi\rangle$ is not entangled of W-type (compare main text). For this, it would suffice by (S13) to verify that the single-particle eigenvalues of the experimentally realized state ρ satisfy the relation

$$\lambda_{\max}^{(1)}(\rho) + \lambda_{\max}^{(2)}(\rho) + \lambda_{\max}^{(3)}(\rho) + \lambda_{\max}^{(4)}(\rho) < 3 - 0.21 = 2.79.$$

For comparison, for the symmetric Dicke state $|D_4^{(2)}\rangle = \frac{1}{\sqrt{6}}(|0011\rangle + |0101\rangle + |0110\rangle + |1001\rangle + |1010\rangle + |1100\rangle)$ the left-hand side of the inequality is equal to 2.

The second, alternative approach for treating noise δ consists in realizing that there exists a function $\delta(p)$ such that if the local eigenvalues are more than $\delta(p)$ away from an entanglement polytope Δ_C , then ρ cannot be written as a convex combination of

pure states $|\phi_i\rangle \in \bar{\mathcal{C}}$. More precisely, define the distance between an experimentally obtained collection of eigenvalues $\lambda(\rho)$ and an entanglement polytope $\Delta_{\mathcal{C}}$ by

$$d(\lambda(\rho), \Delta_{\mathcal{C}}) := \min_{\mu \in \Delta_{\mathcal{C}}} \sum_{k=1}^N \|\vec{\lambda}^{(k)}(\rho) - \vec{\mu}^{(k)}\|_1.$$

Then the desired function $\delta(p)$ is characterized by the property that

$$d(\lambda(\rho), \Delta_{\mathcal{C}}) > \delta(p) \implies \rho \notin \text{conv} \{|\phi\rangle\langle\phi| : \phi \in \bar{\mathcal{C}}\}.$$

A simple estimate can be derived along the lines of the previous paragraph. Indeed, assume that $d(\lambda(\rho), \Delta_{\mathcal{C}}) > \delta(p)$ for some value $\delta(p)$ that is yet to be determined. Let $|\psi\rangle = |\psi_1\rangle$ be as above, and let $|\phi\rangle \in \mathcal{C}$ be arbitrary. Then

$$\| |\psi\rangle\langle\psi| - |\phi\rangle\langle\phi| \|_1 \geq \| |\phi\rangle\langle\phi| - \rho \|_1 - \| \rho - |\psi\rangle\langle\psi| \|_1 > \frac{\delta(p)}{N} - \left(1 - \sqrt{2p-1}\right) =: \varepsilon(p),$$

where the first step is the triangle inequality, and the second step mimics (S11). Borrowing another estimate from (58), this implies that $|\langle\psi|\phi\rangle|^2 < 1 - \frac{1}{4}\varepsilon(p)^2$ for all $|\phi\rangle \in \mathcal{C}$. Now assume for the sake of reaching a contradiction that $\rho = \sum_i r_i |\phi_i\rangle\langle\phi_i|$ can in fact be written as a convex combination of pure states $|\phi_i\rangle$ from \mathcal{C} .

$$\langle\psi|\rho|\psi\rangle = \sum_i r_i |\langle\psi|\phi_i\rangle|^2 < 1 - \frac{1}{4}\varepsilon(p)^2.$$

On the other hand, $\langle\psi|\rho|\psi\rangle \geq p$, which is a contradiction whenever $p \geq 1 - \frac{1}{4}\varepsilon(p)^2$. A short calculations proves that this is certainly the case if we choose $\delta(p) := N(1 + 2\sqrt{1-p} - \sqrt{2p-1})$.

4. Linear Entropy of Entanglement and its Distillation

a. Entanglement Polytopes and the Origin

Pure quantum states $\rho = |\psi\rangle\langle\psi|$, whose one-body reduced density matrices are maximally mixed, i.e., $\rho^{(k)} \propto \mathbb{1}$, play a special role in entanglement theory. First, any such state maximizes the total uncertainty $\sum_j (\Delta R_j)^2$ of any orthonormal basis of local observables R_j (38). Second, any entanglement monotone $M(|\psi\rangle\langle\psi|) := |P(|\psi\rangle)|$ defined in terms of a G -invariant homogeneous polynomial P attains on ρ its maximal value over all the states in the same entanglement class (33, 38). To see this, observe that

$$M(\rho) = |P(|\psi\rangle)| = |P(g|\psi\rangle)| = \|g|\psi\rangle\|^n |P\left(\frac{g|\psi\rangle}{\|g|\psi\rangle}\right)| \geq |P\left(\frac{g|\psi\rangle}{\|g|\psi\rangle}\right)| = M(g \cdot \rho)$$

where n is the degree of P ; the inequality follows from a result by Kempf and Ness which states that $\|g|\psi\rangle\| \geq \| |\psi\rangle \|$ for all $g \in G$ if the $\rho^{(k)}$ are maximally mixed (59).

The point in the entanglement polytopes corresponding to quantum states with maximally mixed one-body reduced density matrices will be called the *origin* and denoted by O ; it satisfies $\vec{\lambda}^{(k)} \propto (1, \dots, 1)$ for all k . Clearly, O cannot be expressed as a proper convex combination of any two other points in the entanglement polytope, for we have arranged each vector of eigenvalues in weakly decreasing order. Therefore, Theorem 1 implies that the origin is contained in the entanglement polytope if and only if there exists a covariant with weights $\vec{\mu}^{(k)} \propto (1, \dots, 1)$. Such a covariant is of course nothing but a G -invariant homogeneous polynomial; hence,

$$O \in \Delta_{\mathcal{C}} \iff \exists \text{ a } G\text{-invariant homogeneous polynomial which is non-zero at } \rho.$$

In particular, any entanglement monotone defined via polynomial invariants necessarily vanishes on those quantum states whose entanglement polytopes do not include the origin (these states are also called *unstable* in geometric invariant theory (60); their complement being the *semi-stable* states). This observation has lead to the suggestion that unstable states should be considered “unentangled” (38) or “not genuinely multipartite entangled” (36, 37), even though they might be entangled according to the standard notion of entanglement that we have adopted in this work.

b. *Linear Entropy of Entanglement*

The geometric picture provided by entanglement polytopes suggests another way of quantifying entanglement, which assigns non-zero values to all entangled states, namely the Euclidean distance of the collection of local eigenvalues. This quantity is precisely equal to the ℓ_2 -norm distance by which the reduced density matrices differ from being maximally mixed. Moreover, it is by an affine transformation related to the multi-particle version of the (*linear*) *entropy of entanglement* (21, 61, 62) given by

$$E(\rho) = E(\vec{\lambda}^{(1)}, \dots, \vec{\lambda}^{(N)}) = 1 - \frac{1}{N} \sum_{k=1}^N \|\vec{\lambda}^{(k)}\|_2^2 = 1 - \frac{1}{N} \sum_{k=1}^N \|\rho^{(k)}\|_2^2.$$

Indeed,

$$\|(\vec{\lambda}^{(1)}, \dots, \vec{\lambda}^{(N)}) - O\|_2^2 = \sum_{k=1}^N \|\rho^{(k)} - \frac{\mathbb{1}}{d_k}\|_2^2 = \sum_{k=1}^N \|\rho^{(k)}\|_2^2 - \frac{1}{d_k} = \left(N - \sum_{k=1}^N \frac{1}{d_k} \right) - NE(\rho). \quad (\text{S14})$$

The linear entropy of entanglement admits an operational interpretation (63); in the case of multiple qubits, it reduces to the Meyer–Wallach measure of entanglement, and to the concurrence in the case of two qubits (64–66).

The following result then follows immediately from convexity. It naturally generalizes the properties satisfied by states with maximally mixed one-body reduced density matrix.

Proposition 3. *Any entanglement polytope $\Delta_{\mathcal{C}}$ contains a unique point of minimal Euclidean distance to the origin O . The corresponding quantum states ρ maximize the linear entropy of entanglement $E(\rho)$ over all states in $\bar{\mathcal{C}}$.*

The maximal entropy of entanglement that can be obtained from states in the closure of the entanglement class \mathcal{C} ,

$$E(\Delta_{\mathcal{C}}) = \max\{E(\rho) : \rho \in \bar{\mathcal{C}}\} = \max\{E(\vec{\lambda}^{(1)}, \dots, \vec{\lambda}^{(N)}) : (\vec{\lambda}^{(1)}, \dots, \vec{\lambda}^{(N)}) \in \Delta_{\mathcal{C}}\}$$

is in view of (S14) a simple function of the Euclidean distance of the entanglement polytope to the origin and can thus be computed easily.

c. *Entanglement Distillation*

Given the linear entropy of entanglement $E(\rho)$ as a means of quantifying multi-particle entanglement, it is natural to ask for a corresponding distillation procedure, i.e., a protocol for transforming the quantum state ρ by SLOCC operations to a state with maximal linear entropy of entanglement. This might only be possible asymptotically, as the maximum might be contained in the boundary of $\bar{\mathcal{C}}$.

The function $E(\rho)$ is smooth and can therefore be maximized locally by following its gradient flow in $\mathcal{C} = G \cdot \rho$. By (S7),

$$dE|_{\rho} = -\frac{2}{N} d\langle \Phi, (\rho^{(1)}, \dots, \rho^{(N)}) \rangle |_{\rho} = -\frac{2}{N} \omega_{\text{FS}}(\widehat{X}_{\rho}, -) = -\frac{2}{N} \text{tr}(\widehat{X}_{\rho} -), \quad (\text{S15})$$

where we denote by \widehat{X}_{ρ} the tangent vector generated at ρ by the infinitesimal action of the collection of reduced density matrices. The last identity holds since $\mathbb{P}(\mathcal{H})$ is a Kähler manifold. Therefore, the gradient of E is at every point $\rho = |\psi\rangle\langle\psi|$ equal to

$$\text{grad } E(\rho) = -\frac{2}{N} \widehat{X}_{\rho} = -\frac{2}{N} \frac{d}{dt} \Big|_{t=0} \frac{(e^{t\rho^{(1)}} \otimes \dots \otimes e^{t\rho^{(N)}}) |\psi\rangle\langle\psi| (e^{t\rho^{(1)}} \otimes \dots \otimes e^{t\rho^{(N)}})}{\|(e^{t\rho^{(1)}} \otimes \dots \otimes e^{t\rho^{(N)}}) |\psi\rangle\|^2}, \quad (\text{S16})$$

which factors over the action (S3) of the Lie algebra of G . Therefore, any solution ρ_t to the gradient flow equation remains in the entanglement class of the initial value $\rho_0 = \rho$ at all times $t > 0$.

In mathematical terms, the Euclidean distance to the origin and hence $E(\rho)$ are closely related to the norm square of the moment map (cf. § 3 b), and the latter is a minimally degenerate Morse function in the sense of Kirwan (27). The corresponding analog of (S16) had already been noticed in (27). Moreover, it was established that while the solution ρ_t of the gradient flow equation might not necessarily converge to a unique limit point, E is sufficiently well-behaved so that $E(\rho_t)$ always converges to the global maximum as $t \rightarrow \infty$. We summarize:

Theorem 4. *By following the gradient flow of E , which at any point ρ is given by the infinitesimal action of the reduced density matrices (S16), the global maximum of the linear entropy of entanglement in the closure of the entanglement class of ρ is reached (possibly asymptotically).*

In practice, the gradient flow in Theorem 4 would need to be implemented with finite time steps. That is, after preparing the quantum state ρ one measures its one-body reduced density matrices, re-prepares and performs local POVM measurements with Kraus operators $S^{(k)} \propto e^{t\rho^{(k)}}$, $F^{(k)} = \sqrt{\mathbb{1} - (S^{(k)})^\dagger S^{(k)}}$ for sufficiently small but finite $t > 0$ (cf. (S2)). If the outcomes of these measurements are $S^{(1)}, \dots, S^{(N)}$ then entanglement has been distilled. By successively repeating this procedure and concatenating the SLOCC operations, one asymptotically arrives at a quantum state with maximal entropy of entanglement. Notably, this method of entanglement distillation only requires local tomography and works on a single copy of the state at a time.

From a theoretical perspective, the limit point $\lim_{t \rightarrow \infty} \rho_t$ of the gradient flow can also be seen as a normal form of the state ρ in its entanglement class (in case this limit exists). This is the point of view taken in (33), where a similar numerical algorithm has been given for the special case where O is contained in the entanglement polytope.

5. Examples

By associating to every entanglement class its entanglement polytopes, we have obtained a finite yet systematic classification of multi-particle entanglement. In this section, we will illustrate their computation and application by a series of examples for systems of several qubits.

Mathematically, the covariants of a multi-qubit system are in one-to-one correspondence with the covariants of binary multilinear forms, whose study is a prominent topic in classical invariant theory (67, 68). Before we proceed, we introduce some notational simplifications. It will be convenient to represent the local eigenvalues of a system of N qubits by the tuple $(\lambda_{\max}^{(1)}, \dots, \lambda_{\max}^{(N)}) \in [1/2, 1]^N$ of *maximal* local eigenvalues. This is of course without loss of information, since the sum of the two eigenvalues of any qubit density matrix, which is a 2×2 positive semidefinite Hermitian matrix of trace one, is equal to unity. Similarly, we may label the weights of a covariant by the tuple $(\mu_{\max}^{(1)}, \dots, \mu_{\max}^{(N)}) \in \{\lceil n/2 \rceil, \dots, n\}^N$, since the sum of the components of each weight $\vec{\mu}^{(k)}$ has been fixed to be equal to the degree n of the covariant.

a. Three Qubits

In the case of three qubits, with Hilbert space $\mathcal{H} = \mathbb{C}^2 \otimes \mathbb{C}^2 \otimes \mathbb{C}^2$, there are six distinct entanglement classes (6): The classes of the GHZ state (7) and of the W state (6),

$$|\text{GHZ}\rangle = \frac{1}{\sqrt{2}}(|\uparrow\uparrow\uparrow\rangle + |\downarrow\downarrow\downarrow\rangle), \quad |W\rangle = \frac{1}{\sqrt{3}}(|\uparrow\uparrow\downarrow\rangle + |\uparrow\downarrow\uparrow\rangle + |\downarrow\uparrow\uparrow\rangle),$$

three classes that correspond to EPR states shared between any two of the three subsystems,

$$|B1\rangle = \frac{1}{\sqrt{2}}(|\uparrow\uparrow\downarrow\rangle - |\uparrow\downarrow\uparrow\rangle), \quad |B2\rangle = \frac{1}{\sqrt{2}}(|\uparrow\uparrow\downarrow\rangle - |\downarrow\uparrow\uparrow\rangle), \quad |B3\rangle = \frac{1}{\sqrt{2}}(|\uparrow\downarrow\uparrow\rangle - |\downarrow\uparrow\uparrow\rangle),$$

and the separable class represented by $|\text{SEP}\rangle = |\uparrow\uparrow\uparrow\rangle$.

We shall now compute the corresponding entanglement polytopes by following the general method of covariants described in § 3 c. Using techniques crafted towards the special situation of three qubits, the same polytopes have already been computed in (18, 69); the corresponding quantum marginal problem, which as we have explained amounts to computing the maximal entanglement polytope, has been solved in (54). A minimal set of generators of the covariants of a three-qubit system (in fact, of the equivalent question for binary three-linear forms), has been determined in late 19th century invariant theory (70): There are six generators, and we have summarized their properties in Table S1. By Theorem 2, computing the entanglement polytopes is now a mechanical task: for any quantum state representing the entanglement class, we merely need to collect those covariants which do not vanish on the state, and take the convex hull of their normalized weights.

The resulting entanglement polytopes are illustrated in Fig. S1. They are in one-to-one correspondence to the six entanglement classes described above; that is, in this particular case there is no coarse-graining. As explained before, one polytope is contained in the other if quantum states in the former class can be approximated arbitrarily well by states in the latter class. In this case, this is also a necessary condition, since there is no coarse-graining. Since the GHZ-class polytope is maximal, it follows that all states can be approximated arbitrarily well by states of GHZ type. In mathematical terms, the GHZ class is dense; this is of course well-known (6). Similarly, the polytope of the W class (upper pyramid) contains all entanglement polytopes *except* the GHZ one, so that by states in the W class one can approximate all states except those of GHZ class.

We now illustrate our method of entanglement witnessing:

- If the point $(\lambda_{\max}^{(1)}, \lambda_{\max}^{(2)}, \lambda_{\max}^{(3)})$ corresponding to the collection of local eigenvalues is contained in the lower part of the GHZ entanglement polytope (Fig. S1, (A)),

$$\lambda_{\max}^{(1)} + \lambda_{\max}^{(2)} + \lambda_{\max}^{(3)} < 2,$$

then it is by (S4) not contained in any other entanglement polytope, and therefore the quantum state at hand must be entangled of GHZ type.

- More generally, if the point is *not* contained in any of the polytopes corresponding to an EPR state shared between two of the three particles (Fig. S1, (c), which includes (d)), i.e., if

$$\lambda_{\max}^{(k)} < 1 \quad (\forall k = 1, 2, 3),$$

then by (S4) the quantum state at hand must be entangled of either GHZ or W classes. These classes of states are the ones that possess genuine three-qubit entanglement.

As a final example, we consider the quantum state $\rho = |\psi\rangle\langle\psi|$, where

$$|\psi\rangle = \frac{1}{\sqrt{7}} (|\uparrow\uparrow\uparrow\rangle + |\uparrow\uparrow\downarrow\rangle + |\downarrow\uparrow\uparrow\rangle + 2|\downarrow\downarrow\uparrow\rangle).$$

It is easy to verify by the method of covariants that the entanglement polytope of ρ is full-dimensional, and by the above classification it follows that ρ is of GHZ type. However, its collection of local eigenvalues, $(\lambda_{\max}^{(1)}, \lambda_{\max}^{(2)}, \lambda_{\max}^{(3)}) \approx (0.76, 0.79, 0.88)$, is contained in the interior of the upper pyramid. As we have just discussed, the entanglement criterion (S4) in this case only allows us to conclude that ρ is of either GHZ or W type. By using the entanglement distillation procedure described in § 4 c we can however transform ρ by into another state whose local eigenvalues are arbitrarily closed to the origin $O = (0.5, 0.5, 0.5)$ (Fig. S2). In this way, we arrive at quantum states which are both more entangled and for which our entanglement criterion (S4) is maximally informative.

b. Four Qubits

The case of three qubits was rather special, since there the entanglement polytopes represent faithfully the hierarchy of closures of the corresponding entanglement classes—no coarse graining takes place. In contrast, for four qubits the situation is the generic one: There are infinitely many entanglement classes. According to the classification of (8), they can be partitioned into nine families with up to four complex continuous parameters each. Neither the families themselves, nor the complex parameters within these families are directly experimentally accessible.

Here, we sketch a proof showing that the polytopal view strikes an attractive balance between reducing the complexity sufficiently to allow for simple experimental criteria on the one hand, and preserving a non-trivial structure on the other hand. Indeed, following the tradition established in (6) and continued in (8), we may state that through the polytopal lense, *four qubits can be entangled in seven different ways*.

We have determined all entanglement polytopes of four qubits using the general method (§ 3 c) applied to a minimal generating set of 170 covariants found in (32). More precisely, for every family in (8), we have analytically computed the covariants using a computer algebra system. Deciding whether a normalized weight $\frac{1}{n_j} \mu_j^{(k)}$ is included in Δ_C then amounts to solving the explicit polynomial equation $P_j(\rho) \neq 0$. The algebra system can readily perform such calculations analytically.

The polytope Δ formed by the marginal eigenvalues of all possible pure states is the convex hull of 12 vertices. These can be easily described as follows: One vertex, $(\lambda_{\max}^{(1)}, \dots, \lambda_{\max}^{(4)}) = (1, 1, 1, 1)$, corresponds to product states; six vertices

$$(0.5, 0.5, 1, 1), (0.5, 1, 0.5, 1), (0.5, 1, 1, 0.5), (1, 0.5, 0.5, 1), (1, 0.5, 1, 0.5), (1, 1, 0.5, 0.5)$$

belong to two-partite entangled states; four vertices

$$(0.5, 0.5, 0.5, 1), (0.5, 0.5, 1, 0.5), (0.5, 1, 0.5, 0.5), (1, 0.5, 0.5, 0.5)$$

to three-partite entangled states, and one vertex $(0.5, 0.5, 0.5, 0.5)$ which is the image of a four-partite entangled state (not necessarily *genuinely* four-partite entangled—see § 5 c). This latter vertex is the origin as defined in § 4 a.

As in the three-qubit case, there are several lower-dimensional subpolytopes corresponding to bi-separable states. These are obtained by embedding the entanglement polytopes found in the previous section into the full four-qubit polytope in the obvious way. All possibilities are listed in Table S2.

We turn to the genuinely four-body entangled states. There are seven such polytopes, all full-dimensional. Their definitions and some of their properties are listed in Table S3 and Fig. S3. The four-qubit *W*-state (or Dicke state) $|W_4\rangle = \frac{1}{\sqrt{4}}(|\uparrow\uparrow\uparrow\downarrow\rangle + |\uparrow\uparrow\downarrow\uparrow\rangle + |\uparrow\downarrow\uparrow\uparrow\rangle + |\downarrow\uparrow\uparrow\uparrow\rangle)$ corresponds to polytope 5. As is the case for three qubits, the polytope is an “upper pyramid”, i.e., it is the intersection of the full polytope Δ with the half-space defined by

$$\lambda_{\max}^{(1)} + \lambda_{\max}^{(2)} + \lambda_{\max}^{(3)} + \lambda_{\max}^{(4)} \geq 3. \quad (\text{S17})$$

Again in analogy to the three-qubit case, we can take any violation of (S17) as an indication of “high entanglement”. One way to make this precise is to read off Table S3 that violations imply that the state $|\psi\rangle$ can be converted into one with entropy of entanglement at least 0.45 (which might be much higher than $E(|\psi\rangle)$ as obtained from the measured data!). The entanglement classes of the four-qubit GHZ state and of the cluster states (71) are associated with the full polytope (number 7).

There is a numerical coincidence between our findings and the ones in (39), where also seven non-biseparable entanglement classes have been identified on four qubits. The two classifications are, however, not identical. Indeed, (39) is based purely on *invariants*, as opposed to the more general *covariant*-theoretic description of our polytopes. As mentioned in § 4, invariants cannot differentiate unstable entangled states from product states. Hence, the 7 classes of (39) must all be semi-stable. However the same is true only for our polytopes 4, 6 and 7. In this sense, the polytope methods yields a finer classification for unstable vectors, whereas (39) provides a better resolution of the stable case.

In summary, up to permutations, there are 12 entanglement polytopes for four qubits, 7 of which belong to genuinely four-partite entangled classes. The numbers increase to 41 and 22, respectively, if distinct permutations are counted separately.

c. N Qubits and Genuine Multipartite Entanglement

In the examples so far, bi-separable states mapped onto polytopes of lower dimension. This is no longer true for $N \geq 6$ particles (for $N = 6$, the entanglement polytope associated with $|GHZ_3\rangle \otimes |GHZ_3\rangle$ is clearly 6-dimensional). However, it remains true that spectral information alone can be used to witness genuine N -qubit entanglement for any N . A general theory of genuine entanglement detection from spectral information will be presented elsewhere. Here, we merely give one example valid for any number N of qubits. The result is stated in the language of (19); see also (4, 30, 72–75) and references therein. Call a vector $|\psi\rangle$ *producible using k -partite entanglement* if it is of the form $|\psi\rangle = |\psi_1\rangle \otimes \cdots \otimes |\psi_m\rangle$, where every $|\psi_i\rangle$ is contained in the tensor product of at most k sites—otherwise, $|\psi\rangle$ is said to contain *genuine $(k + 1)$ -partite entangled*. In particular, the states that contain genuine N -partite entanglement are precisely those which are not *biseparable*, i.e., those which do not factorize with respect to any non-trivial (bi)partition of the subsystems. The reader should not be confused by the fact that some authors use the term “genuine N -partite entanglement” in a different sense; c.f. (36, 37), where semi-stability (in the sense of § 4) is additionally required for “genuine” entanglement.

Recall first that for a system of N qubits the solution of the quantum marginal problem (i.e., the maximal entanglement polytope) is given by the inequalities

$$\lambda_{\min}^{(i)} \leq \sum_{i \neq j} \lambda_{\min}^{(j)} \quad (\text{S18})$$

for the *smallest* local eigenvalues $\lambda_{\min}^{(i)} = 1 - \lambda_{\max}^{(i)} \in [0, 0.5]$ (54). Therefore, the polytope for the class of states that factorize with respect to a given partition $A_1 \cup \dots \cup A_m = \{1, \dots, N\}$ is defined by the constraints

$$\lambda_{\min}^{(i)} \leq \sum_{i \neq j \in A_l} \lambda_{\min}^{(j)} \quad \forall i \in A_k, k = 1, \dots, m \quad (\text{S19})$$

The following lemma shows that information on the local eigenvalues can serve as a witness for genuine k -qubit entanglement (cf. Fig. 3):

Lemma 5. *Let $N \geq 3$ and $k \in \{\lceil N/2 \rceil, \dots, N\}$. For every $\gamma \in (0, 0.5 \frac{N-1}{k-1}]$ the local eigenvalues*

$$(\lambda_{\min}^{(1)}, \dots, \lambda_{\min}^{(N)}) = \left(\gamma \frac{k-1}{N-1}, \frac{\gamma}{N-1}, \dots, \frac{\gamma}{N-1} \right)$$

can originate only from genuinely k -partite entangled (pure) quantum states of N qubits. Conversely, if $k \neq N - 1$ then there exists a realization in terms of a state producible using k -partite entanglement.

Proof. Consider any bipartition $A_1 \cup A_2 = \{1, \dots, N\}$. Without loss of generality, assume that $1 \in A_1$. Then (S19) for $i = k = 1$ reads

$$\gamma \frac{k-1}{N-1} \leq \sum_{1 \neq j \in A_1} \gamma \frac{1}{N-1} = \gamma \frac{|A_1| - 1}{N-1} \quad \Leftrightarrow \quad |A_1| \geq k. \quad (\text{S20})$$

This immediately proves that any $|\psi\rangle$ with the advertised local spectra is genuinely k -partite entangled. For if such a $|\psi\rangle$ factorizes with respect to some partition, then by (S20) at least one factor must comprise at least k sites.

To show that the local eigenvalues can indeed be realized using k -partite entanglement, consider the bipartition $A_1 = \{1, \dots, k\}$, $A_2 = \{k+1, \dots, N\}$. Then (S20) is satisfied, and so are all other inequalities in (S19) for A_1 . The constraints for A_2 are satisfied if and only if $|A_2| \neq 1 \Leftrightarrow k \neq N - 1$, which is true by assumption. \square

In other words, certain correlations between the one-particle reduced density matrices can only be explained by the presence of genuine k -partite entanglement. This result holds in fact for all choices of local dimensions, since we can always reduce to the qubit situation by considering local eigenvalue spectra of rank at most two.

d. Bosons and Fermions

The theory of entanglement polytopes is readily adapted to the case of indistinguishable particles. Here, the Hilbert space is no longer a tensor product, but the symmetric or antisymmetric subspace in $(\mathbb{C}^d)^{\otimes N}$, where d is the local dimension. Since the particles are indistinguishable, all one-body reduced density matrices are equal. Therefore, the entanglement polytope of an entanglement class \mathcal{C} is in the case of indistinguishable particles defined to be

$$\Delta_{\mathcal{C}} = \left\{ \vec{\lambda}^{(1)} : \vec{\lambda}^{(1)} = \vec{\lambda}(\rho^{(1)}), \rho \in \overline{\mathcal{C}} \right\}. \quad (\text{S21})$$

The reduced density matrices can be diagonalized by the coherent action of the group $K = \text{SU}(d)$, and the corresponding group of SLOCC operations is $G = \text{SL}(d)$ (76). Using these definitions, the theory can be developed in precisely the same way as above.

We shall now illustrate this for the case of a system of N indistinguishable two-level systems with bosonic statistics, with Hilbert space $\mathcal{H} = \text{Sym}^N(\mathbb{C}^2) \subseteq (\mathbb{C}^2)^{\otimes N}$. As in the preceding examples, we may represent the vector of local eigenvalues of the one-body reduced density matrix by its maximum. Thus we may think of an entanglement polytope $\Delta_{\mathcal{C}}$ as a line segment or interval in $[0.5, 1]$.

The entanglement polytopes can be computed as above using covariants, which in this case correspond formally to the covariants of binary forms in mathematics; these are again well-studied and explicitly known for small N (67, 77). As a convenient shortcut, we will however use a geometric argument which immediately gives the entanglement polytopes for arbitrary N :

Lemma 6. *For a system of N bosonic qubits, the entanglement polytopes are given by intervals $[\gamma, 1]$ with*

$$\gamma \in \left\{ \frac{1}{2} \right\} \cup \left\{ \frac{N-k}{N} : k = 0, 1, \dots, \lfloor N/2 \rfloor \right\}.$$

Proof. Since the unentangled states are contained in the closure of every entanglement class, every entanglement polytope $\Delta_{\mathcal{C}}$ contains the point 1. The other end point of the interval, which we denote by $\gamma \geq 0.5$, is by (S14) directly related to the maximal entropy of entanglement $E(\Delta_{\mathcal{C}})$, and we need to determine the possible values of γ . First, we observe that since the generalized GHZ state $\frac{1}{\sqrt{2}}(|\uparrow\rangle^{\otimes N} + |\downarrow\rangle^{\otimes N})$ is locally maximally mixed, $\gamma = 0.5$ can always be achieved for arbitrary N . Let us now suppose that $\gamma > 0.5$, i.e., the spectrum of the one-body reduced density matrix is non-degenerate and hence contained in the interior of the set D_{\downarrow} . Let $\rho = |\psi\rangle\langle\psi|$ be a quantum state whose one-body reduced density matrix is a diagonal matrix with first diagonal entry γ . By (S6), γ can only be a vertex of the entanglement polytope if the range of the differential of Φ at ρ is orthogonal to the space of diagonal observables spanned by σ_z (otherwise, γ could be changed infinitesimally, hence would not be a vertex). By (S7), this is the case if and only if $i\widehat{\sigma}_z \rho$ vanishes—in other words, ρ is fixed by the infinitesimal action of $i\sigma_z$ (and hence of any diagonal local operator) and thus $|\psi\rangle$ is an eigenvector of the σ_z -operator. Such states are known as occupation number basis states, or Dicke states (78). It is easy to see that the one-body reduced density matrix of a Dicke state with N_{\uparrow} spins pointing upward and $N_{\downarrow} = N - N_{\uparrow}$ spins pointing downward is equal to $\text{diag}(N_{\uparrow}/N, N_{\downarrow}/N)$; therefore it is mapped into D_{\downarrow} if $N_{\uparrow} \geq N_{\downarrow}$. Finally, we observe that since the one-body reduced density matrix is diagonal and the global state fixed by diagonal local operators, every Dicke state is a maximum of the entanglement distillation procedure from § 4 c. It follows that γ is indeed minimal, hence a vertex of the entanglement polytope. \square

By associating with each of the entanglement polytopes the set of corresponding quantum states, we obtain $\lfloor N/2 \rfloor + 1$ families of quantum states. Each family generically consists of infinitely many entanglement classes, except for the unentangled one ($\gamma = 1$), and it can be characterized operationally by the maximal linear entropy of entanglement $E(\Delta_{\mathcal{C}})$ that can be achieved by states in the family. Furthermore, it follows from the proof of Lemma 6 that the Dicke states for $\gamma > 0.5$ are (up to local unitaries) uniquely characterized by the property that they attain the maximal entropy of entanglement in their entanglement polytope. In contrast, there are generically infinitely many entanglement classes that contain quantum states which are locally maximally mixed (i.e., sent to the origin, corresponding to $\gamma = 0.5$); this follows because for $N \geq 4$ there is more than a single invariant. For example, the four qubit GHZ state and the Dicke state with $N_{\uparrow} = N_{\downarrow} = 2$ are both locally maximally mixed, but in a different entanglement class.

Our second example is a system of three fermions with local rank six, as described by the Hilbert space $\mathcal{H} = \wedge^3 \mathbb{C}^6$. In (20), Borland and Dennis proved that the set of local eigenvalues compatible with a global pure state is constrained by the inequalities

$$\lambda_1 + \lambda_6 = \lambda_2 + \lambda_5 = \lambda_3 + \lambda_4 = 1, \quad \lambda_1 + \lambda_2 \leq \lambda_3 + 1. \quad (\text{S22})$$

Here we write $\lambda_k = \lambda_k^{(1)}$ for the k -th eigenvalue of the one-body reduced density matrix $\rho^{(1)}$, which—following usual conventions in quantum chemistry—is normalized to $\text{tr } \rho^{(1)} = 3$. This is the solution to the quantum marginal problem, which in this context is also known as the *pure-state N -representability problem*. Notably, (S22) describes a three-dimensional convex polytope in six-dimensional Euclidean space (due to the three equality constraints). We may therefore without loss of information work in three-dimensional space by consider its projection onto the largest three eigenvalues, $(\lambda_1, \lambda_2, \lambda_3)$.

In the Borland–Dennis system there are four distinct entanglement classes (79); see also (80, 81). They can be represented by the following states:

$$\begin{aligned}
 |\psi_A\rangle &= \frac{1}{\sqrt{2}} (|1\rangle \wedge |2\rangle \wedge |3\rangle + |4\rangle \wedge |5\rangle \wedge |6\rangle), \\
 |\psi_B\rangle &= \frac{1}{\sqrt{3}} (|1\rangle \wedge |2\rangle \wedge |4\rangle + |1\rangle \wedge |3\rangle \wedge |5\rangle + |2\rangle \wedge |3\rangle \wedge |6\rangle), \\
 |\psi_C\rangle &= \frac{1}{\sqrt{2}} (|1\rangle \wedge (|2\rangle \wedge |3\rangle + |4\rangle \wedge |5\rangle)), \\
 |\psi_D\rangle &= |1\rangle \wedge |2\rangle \wedge |3\rangle.
 \end{aligned} \tag{S23}$$

Observe that $|\psi_C\rangle$ is the antisymmetrization of a biseparable pure state, while the class of $|\psi_D\rangle$ is equal to set of Slater determinants—the fermionic equivalent of a product state. The states $|\psi_A\rangle$ and $|\psi_B\rangle$ are reminiscent of genuinely entangled GHZ and W states for three qubits (cf. § 5 a). This remarkable correspondence between the entanglement classification of the Borland–Dennis setup and the classification of the three-qubit system can be explained precisely in a group-theoretical way (79).

We now describe the corresponding entanglement polytopes (Fig. S4): The polytope of the first class is given by the solution of the quantum marginal problem, (S22), since the class is dense in the set of pure states. The polytope of the second class is obtained by replacing the vertex $(0.5, 0.5, 0.5)$ (the origin) with $(2/3, 2/3, 2/3)$ (the local eigenvalues of the state $|\Psi_B\rangle$). This can be established geometrically by generalizing the argument used in the proof of Lemma 6, cf. (27). The entanglement polytope of the third class is given by a line segment, and the polytope of the class of Slater determinants is given by single point. Thus the correspondence between the Borland–Dennis system and the three-qubit system is also manifest on the level of entanglement polytopes: the fermionic entanglement polytopes appear as the “anti-symmetrization” of the three-qubit polytopes (cf. Fig. S1).

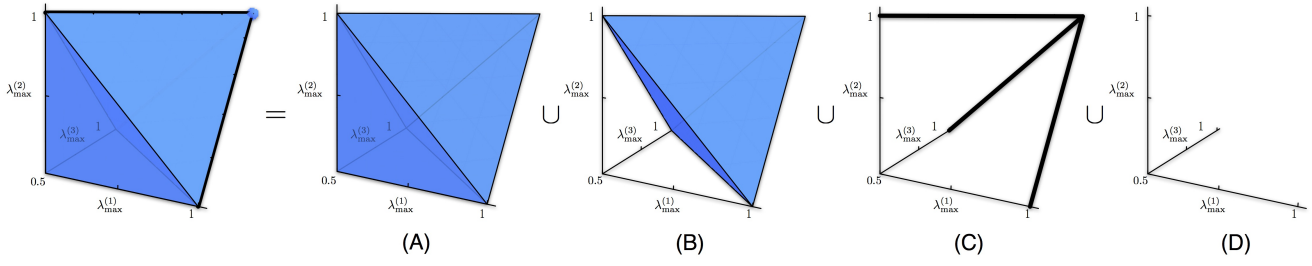


Figure S1. Entanglement polytopes for three qubits: (A) GHZ polytope (entire polytope, i.e., upper and lower pyramid), (B) W polytope (upper pyramid), (C) three polytopes corresponding to EPR pairs shared between any two of the three parties (three solid edges in the interior), (D) polytope of the unentangled states (interior vertex).

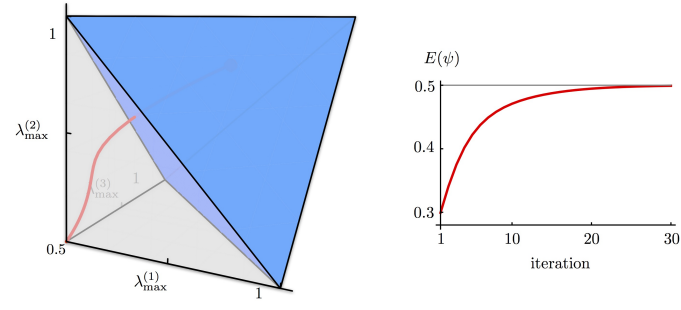


Figure S2. Illustration of entanglement distillation for the quantum state $\rho = |\psi\rangle\langle\psi|$ discussed in § 5 a: by following the gradient flow (curved line), the origin $O = (0.5, 0.5, 0.5)$ is reached asymptotically. The corresponding quantum state has maximal linear entropy of entanglement.

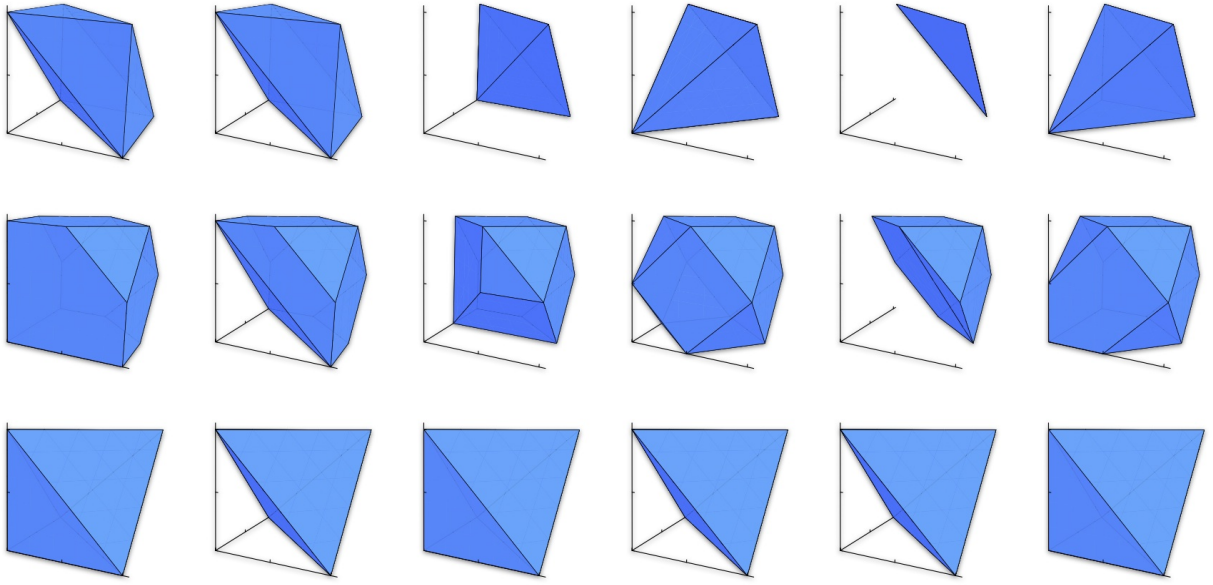


Figure S3. Three-dimensional cuts through the *non-trivial* full-dimensional entanglement polytopes for four qubits. The columns correspond to the first six polytopes in Table S3. The last coordinate is fixed in every row—to values 0.5, 0.75, and 1, respectively, with the remaining three variables shown.

From the first row, one can see that only two of these entanglement polytopes (No. 4 and 6) include the maximally mixed vertex $(0.5, 0.5, 0.5, 0.5)$. These reach the maximal value for the entropy of entanglement. The four polytopes missing the maximally mixed vertex cannot be distinguished from product states using polynomial entanglement monotones (c.f. § 4), showing that our approach is stronger in that regard.

The final row exhibits the behavior of the class when the fourth particle is projected onto a generic pure state. We then recover a three-qubit entanglement polytope on the remaining coordinates. Polytopes 1, 3, and 6 give the full three-qubit polytope implying that a GHZ-type vector is generated. Polytopes 2, 4, and 5 collapse to the upper pyramid of Fig. 1. Hence these entanglement classes produce a W -type state when the first particle is projected onto a pure state. It follows that the mixed 3-tangle (and any other convex-roof extension of a polynomial monotone) vanishes on the mixed state generated by tracing out the last particle of states in these classes. This observation allows us to graphically recover some properties calculated algebraically in (8), such as the vanishing 3-tangle for the class L_{ab_3} , $a = b = 0$ (which corresponds to polytope 5).

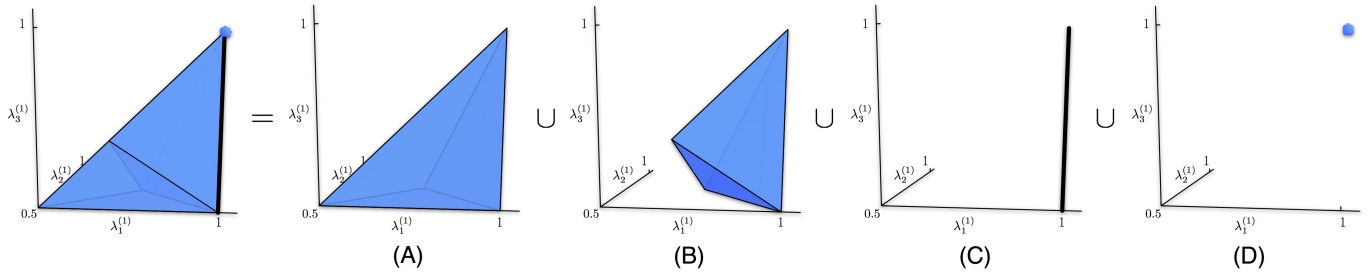


Figure S4. Entanglement polytopes for three fermions with local rank six: (A) class of $|\psi_A\rangle$, (B) class of $|\psi_B\rangle$, (C) class of fermionic “biseparable” states, (D) class of Slater determinants.

Covariant	Degree	Weight	$ \text{GHZ}\rangle$	$ W\rangle$	$ B1\rangle$	$ B2\rangle$	$ B3\rangle$	$ \text{SEP}\rangle$
f	1	(1, 1, 1)	×	×	×	×	×	×
H_x	2	(2, 1, 1)	×	×	×	0	0	0
H_y	2	(1, 2, 1)	×	×	0	×	0	0
H_z	2	(1, 1, 2)	×	×	0	0	×	0
T	3	(2, 2, 2)	×	×	0	0	0	0
Δ	4	(2, 2, 2)	×	0	0	0	0	0

Table S1. Three-qubit covariants—labeled as in (68, p. 33)—with their degree and weight (see § 5 for conventions), and their vanishing behavior on the quantum states representing the six entanglement classes (× denotes non-vanishing). The invariant Δ is Cayley’s hyperdeterminant, which is closely related to the 3-tangle (34, 82).

Representative	Number of embeddings
$ \text{GHZ}\rangle \otimes \uparrow\rangle$	4
$ \text{W}\rangle \otimes \uparrow\rangle$	4
$ \text{EPR}\rangle \otimes \text{EPR}\rangle$	3
$ \text{EPR}\rangle \otimes \uparrow\rangle \otimes \uparrow\rangle$	6
$ \uparrow\rangle \otimes \uparrow\rangle \otimes \uparrow\rangle \otimes \uparrow\rangle$	1

Table S2. Bi-separable classes of four-qubit states. Each class corresponds to an embedding of a three-qubit entanglement polytope from § 5 a into the four-qubit polytope Δ in the obvious way. The right column gives the number of permutations of qubits that lead to distinct embeddings.

No	Family (8)	Parameters	Vertices	Facets	Perms	$E(\Delta_C)$	Vertices compared to full polytope Δ
1	$L_{0_7 \oplus \bar{1}}$		12	13	4	0.482143	(0.5, 0.5, 0.5, 0.5) replaced by (0.75, 0.5, 0.5, 0.5)
2	$L_{0_5 \oplus \bar{3}}$		10	13	4	0.458333	(0.5, 0.5, 0.5, 0.5), (1, 0.5, 0.5, 0.5) missing
3	L_{a_4}	$a = 0$	9	14	6	0.45	(0.5, 0.5, 0.5, 0.5), (0.5, 1, 0.5, 0.5), (0.5, 0.5, 0.5, 1) missing
4	L_{abc_2}	$c = a = -b \neq 0$	8	16	1	0.5	all three-partite entangled vertices missing
5	L_{ab_3}	$b = a = 0$	7	9	1	0.375	all three- and four-partite entangled vertices missing
6	$L_{a_2 b_2}$	$b = -a \neq 0$	10	14	6	0.5	(0.5, 1, 0.5, 0.5), (0.5, 0.5, 0.5, 1) missing
7	G_{abcd}	generic	12	12	1	0.5	n/a — this is the full polytope

Table S3. Entanglement polytopes for genuinely four-partite entangled states. The second column specifies one choice of family and parameters (according to the classification of (8), as corrected in (83)) which gives rise to the polytope shown (there might be further choices, partly because the parametrization of (8) is not always unique). “Perms” is the number of distinct polytopes one obtains when permuting the qubits. As defined in the main text, $E(\Delta_C)$ is the maximal linear entropy of entanglement in the class. The right-most column is a recipe for obtaining the given polytope out of the full one Δ .